POLISH POLAR RESEARCH (POL. POLAR RES.) POLSKIE BADANIA POLARNE	5	1—2	61—97	1984

Andrzej TATUR [1]) and Andrzej BARCZUK [2])

[1]) Department of Biogeochemistry, Institute of Ecology, Polish Academy of Sciences, Dziekanów Leśny, 05-092 Łomianki

[2]) Institute of Mineralogy, Geochemistry and Petrography, Warsaw University, al. Żwirki i Wigury 93, 02-089 Warszawa, Poland.

Phosphates of ornithogenic soils on the volcanic King George Island (Maritime Antarctic)*)

ABSTRACT: Minerals were analysed that had been found in penguin guano and in underlying silicate weathering crust phosphatized by guano leachates. Struvite and hydroxylapatite were found in guano, leucophosphite, minyulite, amorphous aluminum phosphate and taranakite in phosphatized layer, and in some distance from the zone of ornithogenic soils — vivianite. Minerals were identified by the X — ray analysis and results of this identification were confirmed by the microscope studies and the analysis of chemical composition. Results of the thermogravimetric analysis of the selected minerals occurring in monomineral agglomerations (struvite, minyulite, amorphous aluminum phosphate, taranakite) are also presented. Relation between distribution of those minerals in ornithogenic soils and changes in chemical composition of mineral-forming guano leachates during their infiltration through soil, were described.

Key words: Maritime Antarctic, mineralogy, ornithogenic soils, phosphates, phosphatization of silicates

1. Introduction

In the neighbourhood of the bird rookeries located on volcanic rocks, under condition of sufficiently abundant precipitation due to reaction of guano leachates with silicate minerals, very diversified secondary minerals form. The forming mineral phases are mostly aluminum and aluminum — iron phosphates bearing potassium and ammonium (phosphatization process). Those minerals are usually cryptocrystalline and common use of X — ray diffraction methods made possible the investigation of their structure.

*) This work was supported by the Polish Academy of Sciences within the MR-II-16 MR-I-29A Projects carried out at the Arctowski Station during the Fourth Antarctic Expedition 1979/1980.

An attempt of nomenclature systematization of the previously known aluminum-iron phosphates bearing potassium and ammonium was initiated by Bannister and Hutchinson (1947). Principles of systematics of those minerals were proposed by Haseman et al. (1950a, b) during the fundamental pedologic studies. Those authors experimentally analysed the possibility of reaction between phosphate ions and soil silicates under variable physico-chemical conditions (Haseman 1950 a), and next they obtained by immediate solution reactions all the main species of the minerals under consideration (Haseman 1950b). The published X — ray patterns and optical properties of the obtained eighteen various products of precipitation were the basis of distinguishing of the nine fundamental systematic groups. The supplements to those proposals may be found in the paper by Smith and Brown (1959).

The distracted informations concerning occurrence of phosphatized rocks accompanying guano beds were collected by Hutchinson (1950) and White and Warin (1964) but only the Altschuler's (1973) paper brought generalizations on their mineralogy.

2. The area of the studies

The investigations were performed during the Antarctic summer 1979/1980 in the region of the Admiralty Bay on King George Island (Fig. 1), Maritime Antarctic. This island has relatively soft climate as for the neighbourhood of the Continental Antarctic. Average annual temperature equals — 3.9 °C (summer average — 1.1 °C, winter average -6.7 °C). The cloudiness is almost continuous here and days without precipitation are scarce during a year. Annual precipitation exceeds 800 mm and is distributed realtively uniformly in the season. Air humidity is high and averages to 84 per cent (Moczydłowski 1978, Zubek 1981).

During the season 1979/1980 on the ice-free patches of the Admiralty Bay shore, forty-five thousand of penguin couples of the genus *Pygoscelis* nested (Jabłoński 1984). They assembled in several rookeries. Areas of the largest rookeries (presented in Fig. 2—5) were the main field of studies. Penguins nest both on the exposed shore rocks (Fig. 4) and on the inland rocks separated from the sea by zone of crust of loose sedimentary rocks like stony moraine clays, stony deluvia or stony and sandy raised beaches (Fig. 2 and 3). Those rocks under action of the guano leachates use to be intensively phosphatized, that results in characteristic vertical zonality, described in soil science cathegories in the paper by Tatur and Myrcha (1984).

Mainly tertiary basalts and andesites and their tuffs are volcanites that formed the island (Birkenmajer 1980). Such rocks occur as the bedrock in the area of the studied penguin rookeries. Detritus of the same but

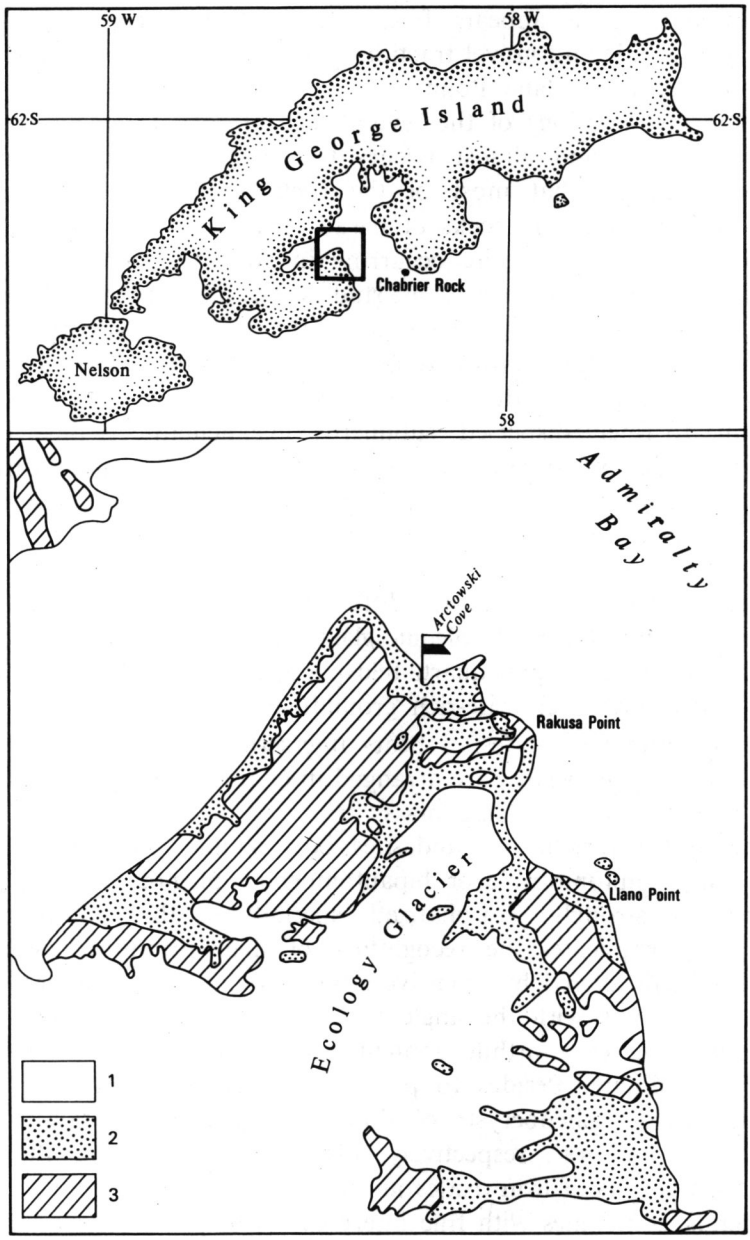

Fig. 1. Sketch map of King George Island with marked ice-free areas after Birkenmajer (1981) simplified by the authors and investigated penguin rookeries near Rakusa Point and Llano Point und on Chabrier Rock

1- ice, 2-Quaternary cover, 3- solid rocks

weathered rocks occurs in the loose sedimentary rocks surrounding the penguin rookery, as it appears from the detailed petrographic analysis performed for pebble and gravel fractions of the phosphatized moraine beds around rookeries near Llano Point.

From the investigations of the several tens of rock fragments from the Llano Point region and almost twenty thin sections from this material there was concluded that most of the rock fragments is andesite and only individual samples are rocks of basalt type.

Several varieties of andesite occurring in rock fragments were distinguished during polarization microscope studies. The differences concern mostly the kind of rock groundmass. Andesites with the vitrophyric (glassy) groundmass, locally weakly devitrified are the first variety. The groundmass frequently is either greenish due to numerous chlorite crystals, or dark-brown to black due to finely dispersed, submicroscopic hematite grains. The two minerals, hematite and chlorites (presence of the latter was confirmed by the X — ray determination), are seemingly the products of decomposition and weathering of certain femic minerals, like biotites, pyroxenes and amphiboles.

The second variety of andesites differs from the first one only in the higher devitrification degree of volcanic glass. This devitrification is presented by numerous fine xenomorphic quartz-feldspar aggregates and granular opaque minerals in vitrophyric, chlorite-rich groundmass.

The third variety of andesites bears intersertal groundmass. Numerous very fine acicular plagioclases are arranged in characteristic polygons, mostly triangles, in vitrophyric or felsic mass.

All the above varieties of andesites bear similar phenocrysts, almost exclusively large, automorphic or hipautomorphic plagioclases. Usually the plagioclases are strongly phosphatized, specially in the central parts of crystals. This complicates the recognition of their primitive composition, on the other hand altered by intensive albitization. Rare less altered plagioclases are oligoclases with the angle $010/\alpha'$ ranging from 0° to -5° and thus corresponding to anorthite content from 10 to 20%. Andesine up to An 40 is subordinate. Besides to plagioclases the studied rock fragments bear relatively rare phenocrysts of diopside augite and basalt augite of angles Z/γ 40° and 49°, respectively. Moreover, there occur the brown, cluster pseudomorphs of iron oxides and/or hydroxides after undeterminable femic minerals, sometimes with fine intergrowths of poorly-crystalline, dark-green chlorite.

Generally, the fragments of those weakly phosphatized andesites have only slightly altered matrix but strongly altered phenocrysts. Fragments of strongly phosphatized andesites although being the rock varieties similar to the described above, consist besides of altered phenocrysts also of intensively altered groundmass. Groundmass, devitrified in various degree,

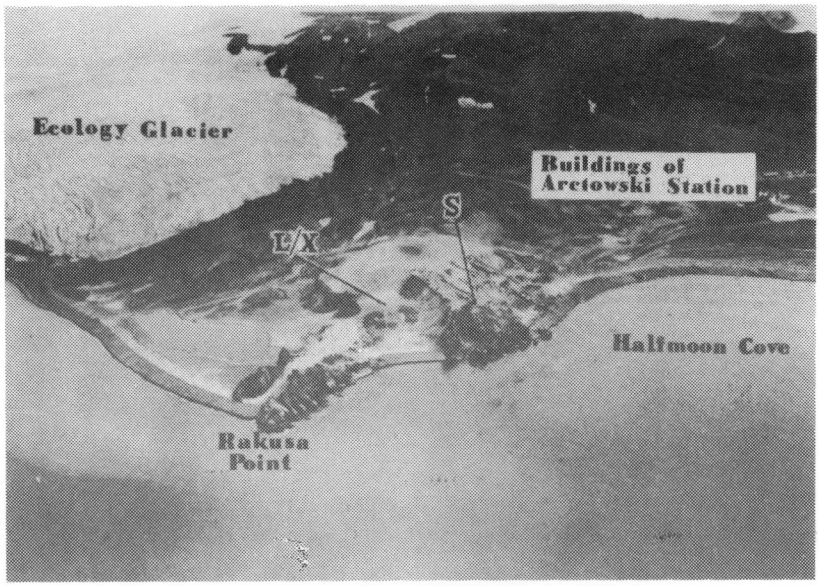

Fig. 2. "Point Thomas" penguin rookery near Rakusa Point
Nesting area is surrounded with light-coloured band of dry guano; S — struvite finding place, L/x — place of sampling of leucophosphite with 8,9 Å, X — ray reflection mineral.

Photo. K. Furmańczyk

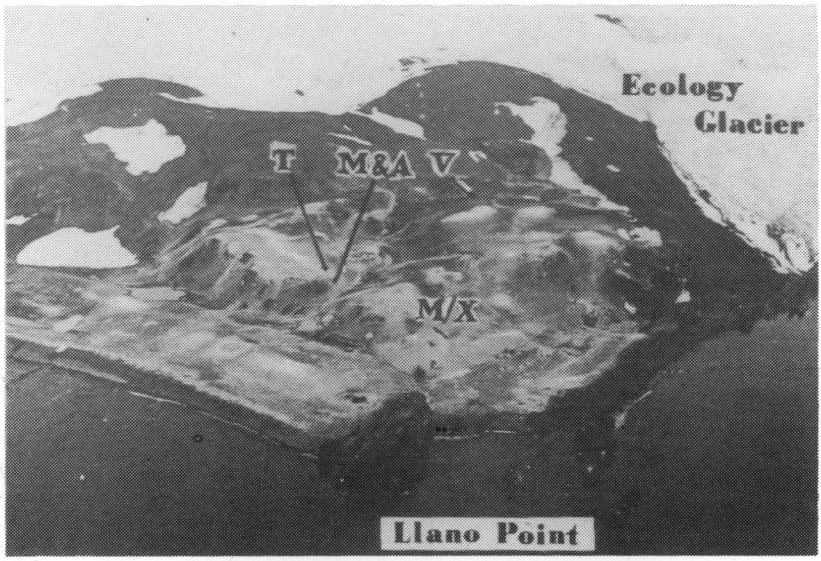

Fig. 3. Penguin rookery near Llano Point
Nesting area is surrounded with light-coloured band of dry guano; M — minyulite finding place depth 15—90 cm, A — amorphous aluminium phosphate finding place depth 70—95 cm, T — taranakite finding place depth below 120 cm, V — vivianite finding place depth 50—150 cm, M/x — place of sampling of minyulite with 8,9 Å X-ray reflection mineral depth 10—70 cm

Photo K. Furmańczyk

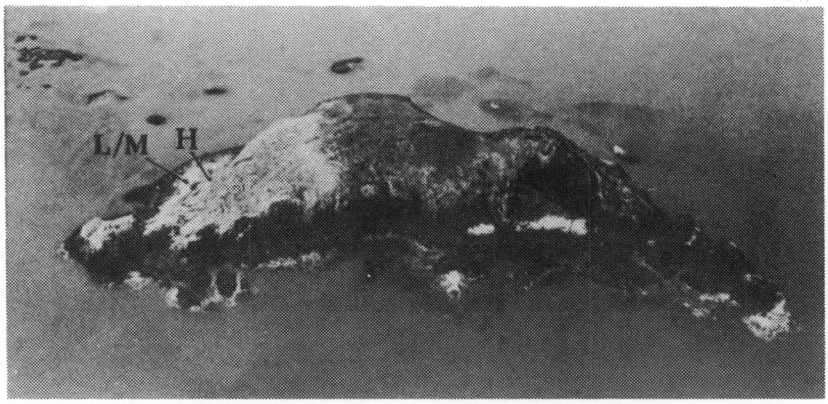

Fig. 4. Penguin rookery on Chabrier Rock
Nesting area is surrounded with light-coloured band of dry guano; L/M place of sampling of leucophosphite with minyulite, H — place of sampling of hydroxylapatite.

Photo K. Furmańczyk

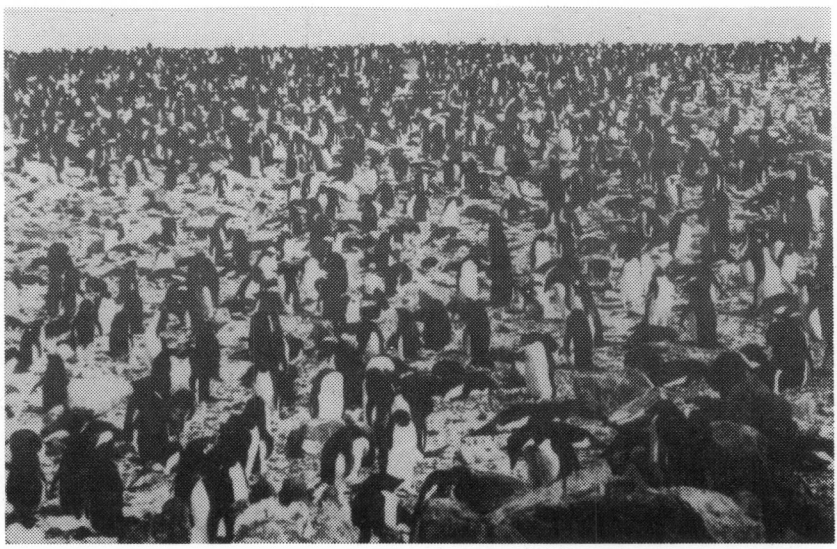

Fig. 5. Area of the vast Adelie penguin rookery near Point Thomas

Photo H. Jackowska

is dark-brown or sometimes even black, and poorly transparent. These features of groundmass are caused by finely dispersed, very abundant products of phosphatization and weathering, very difficult to identification due to minute size of their particles. Locally this groundmass is greenish, probably for reason of the presence of very fine intergrowths and inclusions of chlorite. Granular opaque minerals are quite common. Phenocrysts are weakly altered usually automorphic, zonal plagioclases. Individual recurrent zones are narrow and fine. Plagioclase composition ranges from oligoclase (average An 23) to labrador (average An 52), but andesine about An 40 is the most common plagioclase. Those plagioclases are weakly phosphatized, although there were found rock fragments with the stronger phosphatization, especially of the phenocryst inner core, richer in anorthite component. Complete phosphate pseudomorphs after plagioclases occur exceptionally. Basalt and diopside augites are the other but rare phenocryste, moreover, uralite-chlorite pseudomorphs after femic minerals, presumably amphiboles and pyroxenes, are quite common. Iron oxide/hydroxide pseudomorphs after femic minerals were found exceptionally in this type of rock fragments.

The basalt-type rock fragments have felsic microcrystalline groundmass, consisting of very fine, xenomorphic aggregates of quartz and feldspars, less common chlorites and granular opaque minerals. Hipautomorphic, weakly altered (chloritization and uralitization) basalt augites with the angle Z/γ ranging about 50° and phosphatized plagioclases of anorthite content difficult to determination are the prevailing phenocrysts. Chlorite-iron oxide/hydroxide pseudomorphs after femic minerals are less numerous and serpentine-iddingsite pseudomorphs after olivine, frequently with dark-brown iron compound rims, are rare.

3. Methods

In the paper written by Tatur and Myrcha (1983) the ornithogenic soils near Llano Point were described in details. Phosphates belong to the mineral components occurring in stony loams forming those soils. In certain places the accumulations of exceptionally pure phosphates were found. Thus, one may suppose that those accumulations are monomineral. Mineralogical analysis of those phosphates is discussed in the present paper. Identification of the pure, standard phosphates made possible the determination of mineral composition of polyphase phosphate-silicate mixtures, commonly occurring in the described ornithogenic soils.

Chemical analysis of phosphates was made from the air-dried samples. After initial mineralization of the ground samples at temperature below 500°C, the samples were decomposed by boiling for 30 minutes in HCl and HNO_3 mixture (Belpol'skij et al. 1974). The part of sample insoluble

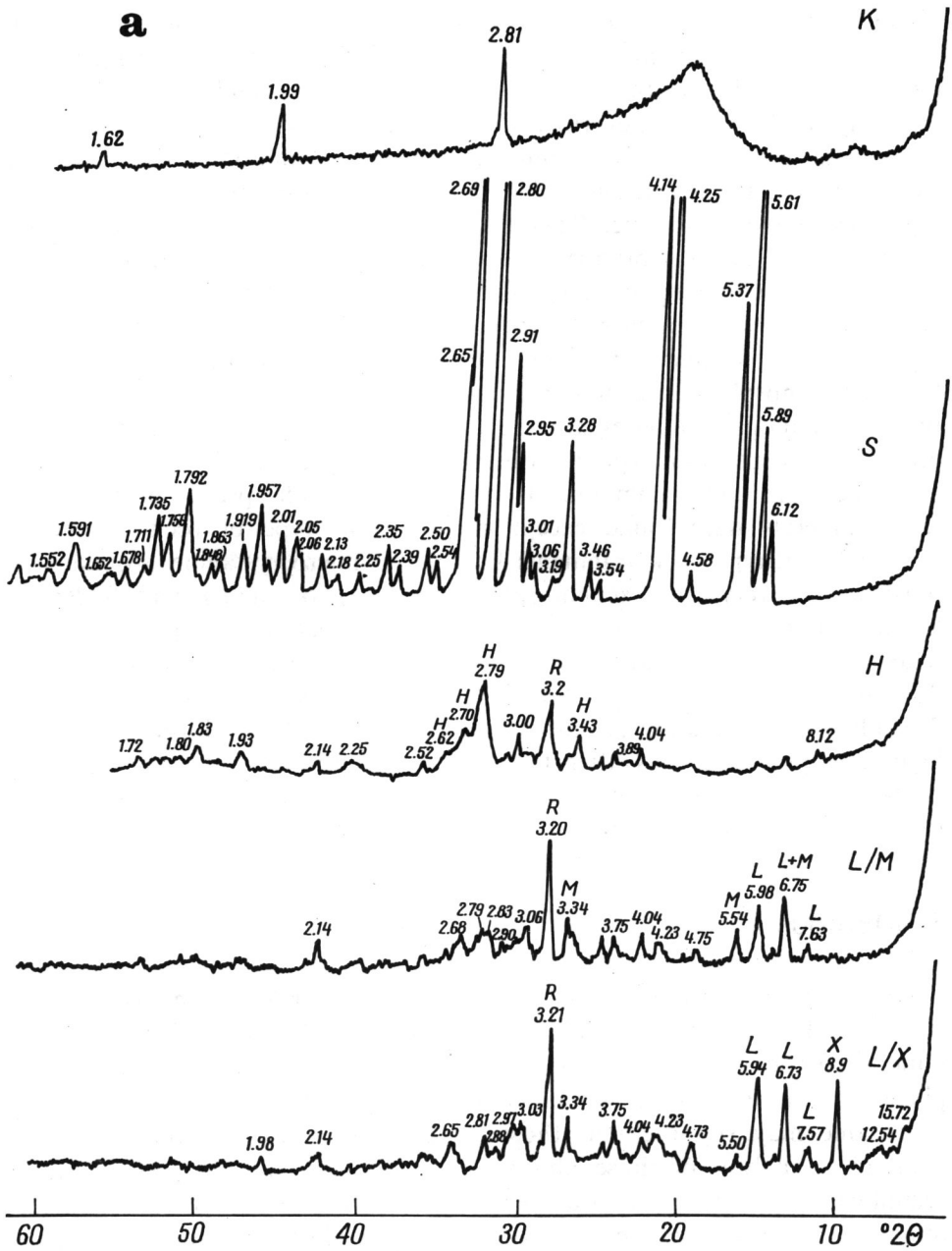

Fig. 6. The X-ray diffraction patterns of ornithogenic phosphates and coexisting minerals
In the diffractograms of the polyphase samples the letters mark only selected reflections, specific for the individual components; K — krill with halite, S — struvite, H — hydroxylapatite (H) on the silicate background (R) and with the small admixture of leucophosphite (L), L/M — leucophosphite (L) with minyulite (M) on the silicate background (R) and with the small admixture of and hydroxylapatite (H), L/X — leucophosphite (L) and phase

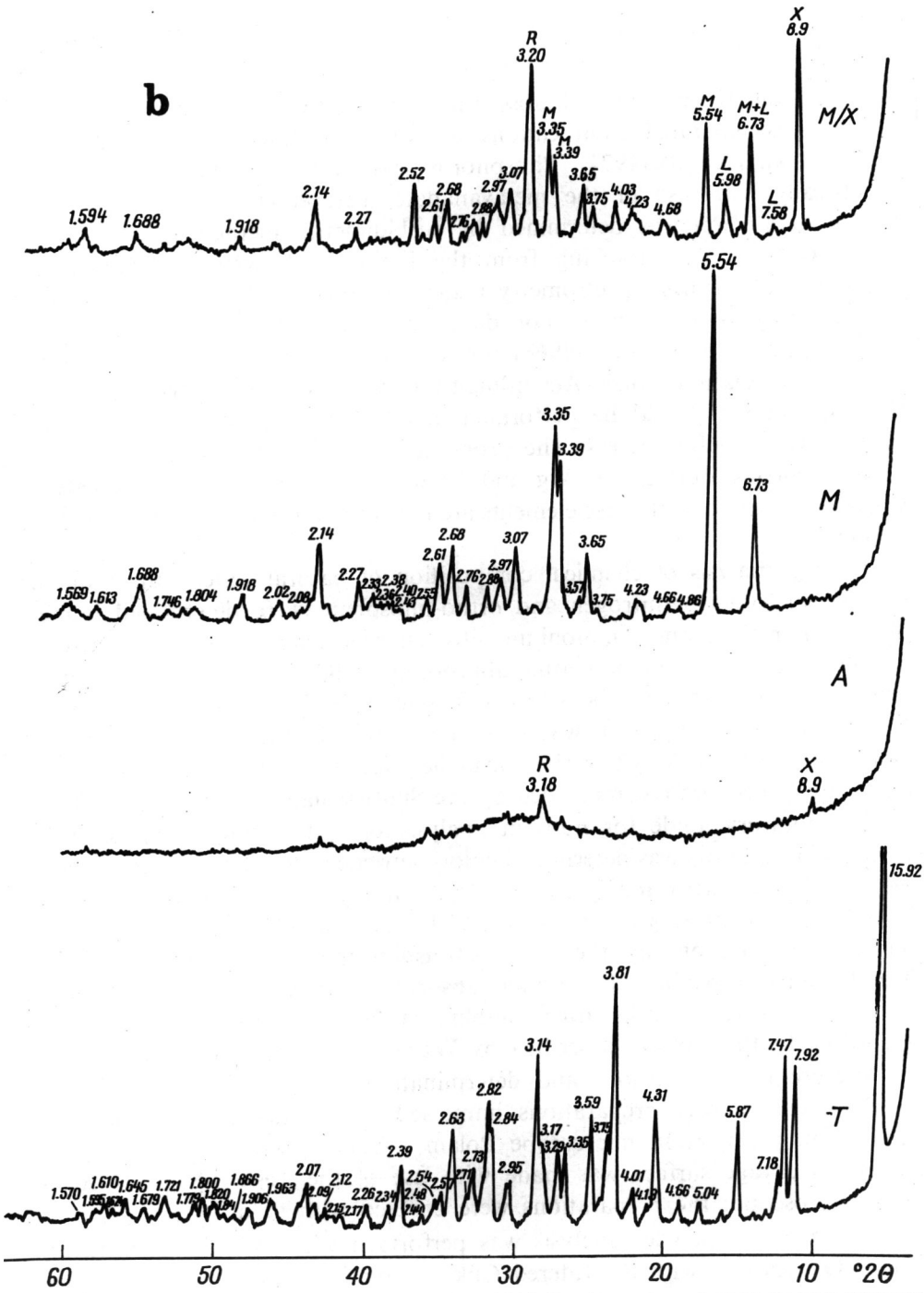

X with the strong reflection 8,9 Å on the silicate background (R) and the small admixture of leucophosphite (L). M — minyulite, A — amorphous aluminum phosphate with small amount of silicates (R), T — taranakite.

Note: numerical values of intensities of individual reflections in monomineral samples of struvite, minyulite and taranakite measured by the planimetric method, are presented in the paper of Tatur and Barczuk (in press).

in acids was filtered on cellulose filter, next dried and weighted. Phosphorus was separated from cations by ionite treatment, as described by Belopol'skij et al. (1974). Phosphorus was determined in leachate colorimetrically with use of the metavanadate method (Belopol'skij et al. 1974). Sulfate ion was determined by turbidimetric method (Marczenko 1979). Cations after leaching from the ionite used, were determined by the atomic absorption spectrometry under conditions described by Rantala and Loring (1975), almost not differing from conditions recommended by Langmyhr and Paus (1968) for analysis of solutions of composition similar to the discussed ones. According to those authors, the determinations of Ca, Mg and Sr should be performed in the N_2O — acetylene flame with the potassium buffer excess. The proposed method minimalizes the interference occurring during Ca, Mg and Sr determination, especially apparent when concentrations of those elements are low and concentration of aluminum is high.

During analysis of chemical composition of natural waters, the mineral (inorganic) forms of nitrogen and ortho-phosphate were determined immediately after sampling. Ammonium nitrogen was determined by the colorimetric hypochlorite method after appropriate dilution, applying the modification of the Solorzano's method (1963) made by Dowgiałło (pers. comm.) Nitrate and nitrite nitrogen was determined colorimetrically with α-napthylamine. Nitrate nitrogen after reduction in the column filled by cadmium (according to the procedure recommended by the Smithsonian Institution in 1978 in the "Laboratory guide for nutrient analysis of water, soil and plant material"). Phosphorus was determined colorimetrically by the molybdenum blue method (Strickland and Person 1968). Chlorides were determined by the turbidimetric method (Marczenko 1979), and soluble carbon, after evaporation of solution, by the wet combustion method (Maciołek 1972). Metals were determined by atomic absorption spectrometry in preserved solutions in three months after sampling, Calcium as well as magnesium according to the method described by Ward and Biechler (1975).

Microscope observations and determinations were preformed with use of the loose powder preparations immersed in Canada balsam and thin sections in polarisation microscope Polam L-211. A series of observations of fresh cleavage surface was made with use of the Tesla PS — 300 scanning microscope; the preparations were covered with gold.

The X — ray powder analysis was performed with use of the diffractometer DRON — 1 with the filtered Cuk α radiation, anode current voltage 38 mV, intensity 10 mA (Fig. 6). The thermogravimetric analysis was made in the device D-1500-Q, MOM Budapest production, in ceramic crucibles with inert reference substance Al_2O_3. Temperature increment rate was 10°/min, sensitivities DTA 250 mA, DTG 1 mA, recording tape velocity 2,5 mm/min (Fig. 7)

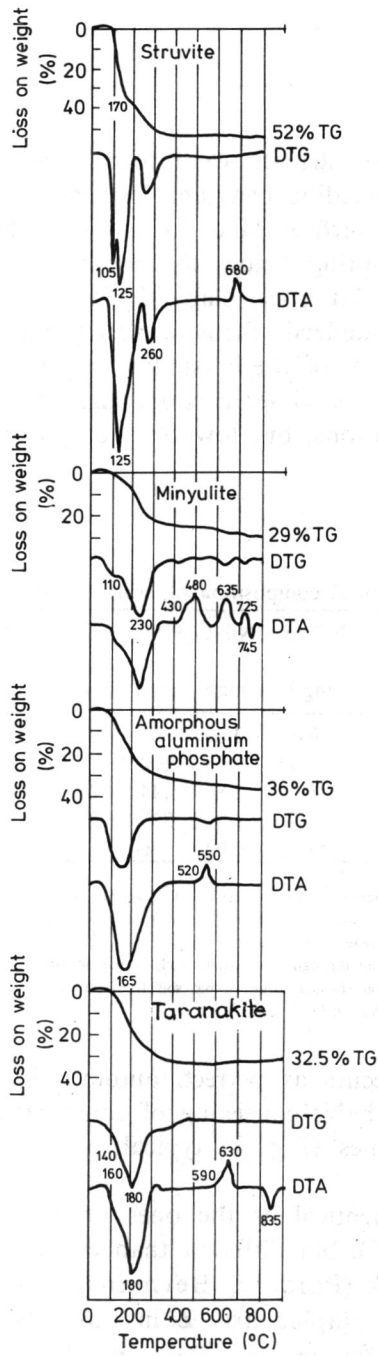

Fig. 7. Results of the thermographic analysis of struvite, minyulite, amorphous aluminum phosphate and taranakite

4. Results

4.1. Struvite

Accumulates of pure struvite were found only in one place. Waters running off from the breeding penguins rookery near Thomas Point, after filtration through the surface layer of soil in the rookery area, next flowed out from the spring below the rookery (Fig. 2). Slowly flowing waters moistured the flat rock slab of the surface about 1 m^2 and here pure struvite crystallized. Struvite accumulated as a few-centimeter wide layer of loose gravel of the crystalline aggregates. Water, from which struvite crystallized, had alkaline reaction, high total salt content and high ammonia ion concentrations, but low ones of phosphorus and magnesium (Table I).

Table I.

Chemical composition of ornithogenic waters

origin of water	pH	N/NH_2 mg/l	N/NO_3 mg/l	N/NO_2 mg/l	P/PO_4 mg/l	Ca mg/l	Mg mg/l	C org. dissolve mg/l	Cl^- mg/l	Conducti vity µS
A	⩾7.4	7000	0.05	0.06	300					
B	⩾7.4	365	0.04	0.05	100					2820
C	⩾7.4	360	48	2.8	44	24	16	16	568	2140
D	4.0	450	157	1.8	220	22	65	80	161	808
E	4.0	4	43	0.02	6			<3		320

A—surface run-off from the penguins rookery (Tatur and Myrcha 1983)
B—surface run-off at the foot of the hill occupied by penguins (Tatur and Myrcha 1983)
C—surface water in place of struvite crystallization
D—ground water (after percolation through ornithogenic soil) in the bottom of the profile No. 5.
E—waters which after percolation through ornithogenic soil from stream in dry period when area of penguins rookery is dry (Tatur and Myrcha 1983)

Struvite ussually occurs as perfect, automorphic crystals orthorhombic symmetry and tabular habit consisting of combination of pedion, pinacoid and orhtorhombic domes (Fig. 8) typical of the class of orthorhombic pyramid.

These forms are identical as the ones presented for struvite in Penkala's handbook (1977), but different than examples shown in the Dana's mineralogical handbook (Palache, Berman and Frondel 1951). The direction of the crystallographic axis Z in this class is determined by the line perpendicular to the pedion {001}, in the studied crystal being in agreement with the optic vector $n\beta$. Optic axes plane is then parallel to the face {001} and next one may accept after Larsen and Bergman (1958) that the X axis agrees with $n\alpha$ vector and the Y axis with $n\gamma$ vector.

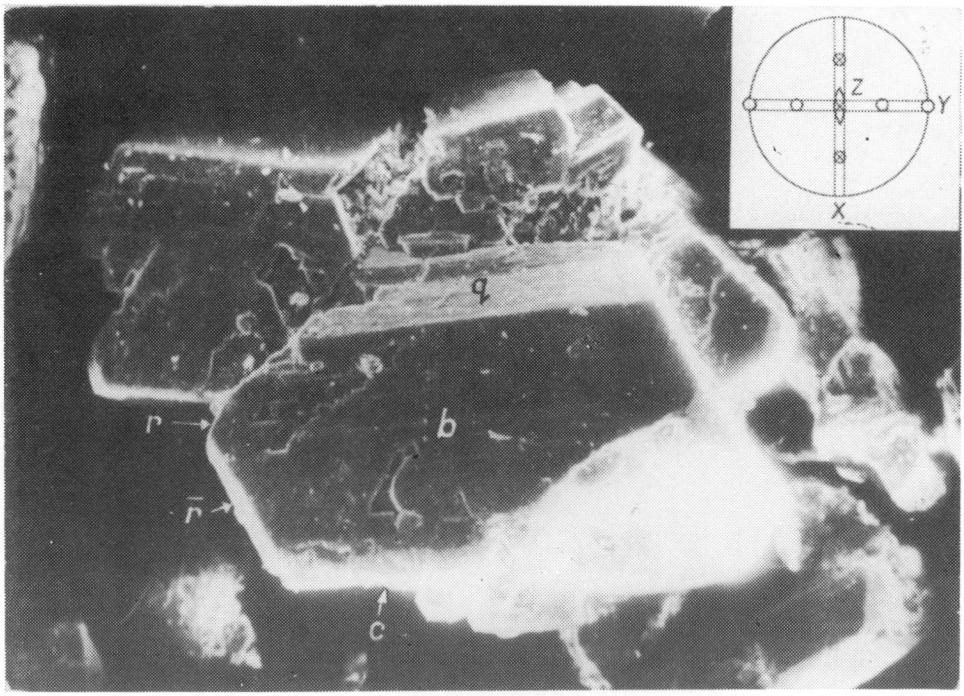

Fig. 8. Aggregates of struvite crystals with the marked crystallographic faces
Scanning electron microscops image, magnification 145x; b — {010} the second pinacoid, r — {101} the transversal upper dome of the second order, r — {101} the transversal lower dome of the second order, q — {011} the transversal upper dome of the first order, c — {001} the lower pedion

Photo A. Tatur, A. Barczuk

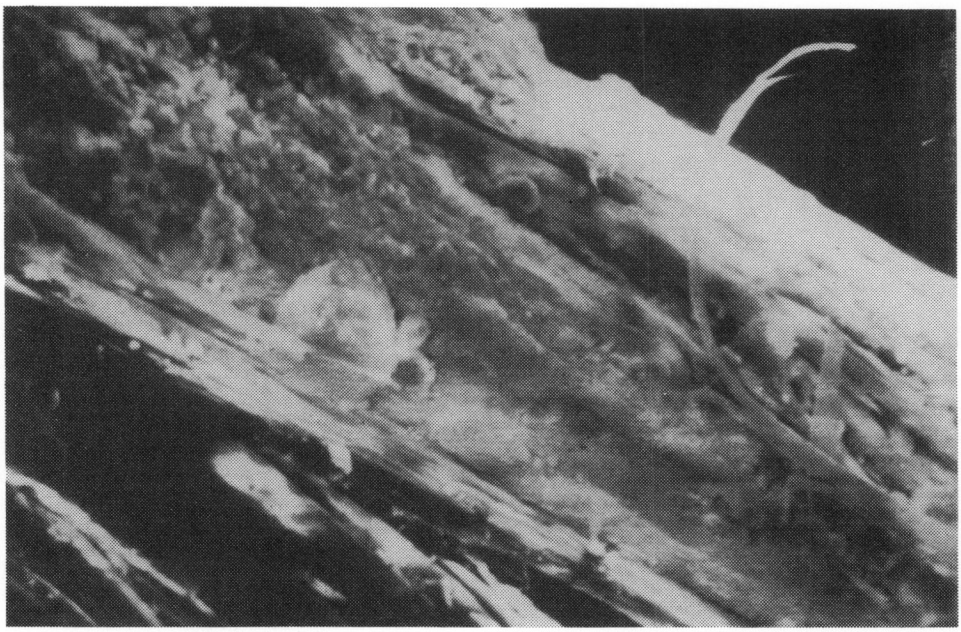

Fig. 9. Hydroxylapatite
Homogeneous, fine-grain phosphate aggregates occurring between fibrous bundles of the chitinous krill remnants. Scanning electron microscope image, magnification 200 x.

This optic orientation is different than that presented by Dana. Tabular flattening (Fig. 8) visible in most crystals occurs along the pinacoid {010} plane, and this causes that identical forms as presented by Penkala finally give the tabular habit differing from the standard crystal habit shown by this author. Cleavage typical of struvite is parallel to the {001} pedion and it is visible (Fig. 8). Most of crystals are several tenths of millimeter long, but individual crystals may reach few millimeters in length. Accretion of struvite crystals according to the face (010) is frequent, resulting in aggregates of the size; twins after the face (001) are relatively rare. Struvite is colorless, non-pleochroic mineral, although abundant gas-liquid and mineral inclusions may cause an accidental color of crystals: brown, gray or black, depending on the inclusion type. Frequently inclusions outline the growth zones of crystals. Usually outer zones of crystals are clear and inclusion-free. Refractive index of struvite ranges from 1.49 for $n\alpha$ to 1.50 for $n\gamma$, similarly as published by Palache, Berman and Frondel (1951) Light extinction in struvite is parallel and birefrigence equals 0.01. The mineral is biaxial positive ($n\gamma$ is the acute bisectrix) with small optic axes angle about 35° and negative sign of elongation.

The X — ray determination of pure struvite (Fig. 6) makes possible its unambiguous identification on the basis of the standard pattern (Swanson et al. 1964). In details the obtained diffractogram is identical with the standard one, made under the same conditions and with use of the same apparatus (Szpila et al. 1982).

The performed chemical analysis revealed certain deviation from the generally accepted formula $Mg(NH_4)PO_4 \times 6H_2O$. Some prevailence of Mg ower NH_4 (Table II) was found, what may suggest the alteration of part of struvite in nitrogen-free newberite (Bridge 1971). The X — ray analysis did not detect any trace of other crystalline phases, including chemically similar phosphates, but it had been performed from the same ground material several months before chemical analysis was made. Partial alteration in newberite might take place during storage of the ground sample waiting for chemical analysis (Bridge 1971). Chemical analysis of struvite performed in the sampling place from the newly collected material detected 6,0 wt. % of nitrogen (Tatur, unpublished data), i.e. amount even exceeding the theoretical content of this element in pure struvite.

In chemical composition of the investigated struvite the high content of manganese isomorphically substituting magnesium, is apparent. This agrees with the earlier observations. However, the found manganese concentration is almost two times higher than the content of manganese reported by Bridge (1971) for struvite that formed under comparable conditions in Skipton Cave, Australia, but there are known also struvite specimens with MnO reaching 2% (Palache, Berman and Frondel 1951).

On the DTA curves (Fig. 7) the two-stage dehydratation is recorded

Table I

Chemical composition of phosphates

	K	S	H	L/M
P_2O_5	4.03	28.51	18.24	—
CaO	1.37	0.57	15.26	6.72
Al_2O_3	0.04	0.00	15.26	8.69
Fe_2O_3	0.04	0.16	4.43	8.29
K_2O	0.84	0.07	0.27	1.38
MgO	0.76	17.80	0.47	0.58
Na_2O	4.19	0.11	2.34	0.84
SrO	0.021	0.00	0.27	0.09
MnO	0.021	0.370	0.04	0.06
ZnO	0.002	0.000	0.033	0.01
CuO	0.0027	0.001	0.031	0.02
TiO_2		0.00	0.05	0.01
insoluble	1.55	13.53	27.74	
loss on weight 600°C			38.38	23.20
sum		100.7	98.10	98.95
loss on weight 110°C		44.21	6.65	—
C		1.17	18.16	6.32
N		5.14	2.86	1.72
H		4.96	2.47	1.80
S		0.01	0.65	
Molar ratios P		1	3	2
N		0.92	—	0.82
Mg		1.10	—	—
Al	—	—	—	1.13
Fe		—	—	0.52
K		—	—	0.20
Mn		0.01	—	—
Ca		—	3.12	—
H		12.25	—	—

Description of the samples:
K — krill sample with halite
S — pure struvite
H — sample of guano with high hydroxylapatite content
L/M — sample of phosphatic, clay with high content of leucophosphite and minyulite
L/X — sample of phosphatic clay with high content of leucophosphite and undefined mineral with 8.9 Å pattern
M/X — sample of phosphatic clay with high content of minyulite and undefined mineral with 8.9 Å pattern
M — pure minyulite
A — almost pure emorphous aluminium phosphate
T — pure taranakite
R — rock

at temperatures 105°C and 125°C with the total mass decrease about 40 wt. %. Endothermic reaction with maximum at temperature 260°C and mass loss about 10% means most probably the NH_3 volatilization. Exothermic reaction with maximum at 680°C without mass loss probably is connected with a sample recrystallization still not recognized sufficiently.

L/x	M/x	M	T	A	R
16.77	17.40	31.53	40.88	25.65	
0.27	1.19	0.77	0.14	2.10	3.50
10.00	10.96	22.30	18.50	20.41	24.57
9.44	3.43	0.69	1.40	1.44	6.44
1.26	4.70	11.20	6.38	1.18	2.65
0.35	0.18	0.22	0.07	0.22	2.85
0.16	0.32	0.41	0.22	0.49	
0.01	0.01	0.06	0.00	0.22	
0.015	0.02	0.005	0.000	0.015	0.13
0.014	0.13	0.02	0.000	0.019	
0.021	0.01	0.041	0.015	0.048	
0.12	0.13	0.05	0.03	0.05	—
43.60	40.92	4.40	1.75	10.24	49(SiO_2)
18.25	17.40	27.06	32.01	36.34	
100.28	96.80	98.76	101.40	98.42	
—	—	6.77	24.01	21.64	
2.48	4.10	4.61	2.59	6.36	
1.41	0.96	0.99	1.35	0.92	
2.02	2.12	2.60	3.66	3.48	
		0.18	0.06	0.23	
2	2	2	8	1	
0.97	0.56	0.32	1.34	—	
—	—	—	—	—	
1.66	1.75	1.97	5.05	1.11	
1.00	0.35	0.04	0.24	—	
0.23	0.81	1.07	1.88	—	
—	—	—	—	—	
—	—	—	—	—	
—	—	11.59	50.43	9.53	

4.2. Hydroxylapatite

In soil at the rookery area, especially in somewhat deeper layer of guano, hydroxylapatite is the common mineral. It occurs also in the thin (1—2 cm) guano layer transported by rainfall water and deposited on the soil surface around the rookery. Hydroxylapatite does not form monomineral accumulation but cryptocrystalline earthy mass among mineral and organic detritus. In scanning microscope the homogeneous, earthy phosphate aggregates are visible, occurring loosely or between the fibrous bundles of the chitinous remains of krill (Fig. 9). Nowhere in the phosphate mass the automorphic crystals were found. The internal structure of aggregates may

be observed frequently as the irregular stratification that developed usually on fine organic detritus from dripping water solution (Fig. 10).

Hydroxylapatite $Ca_5(PO_4)_3OH$ was identified in the sample H. All reflections with intensity over 0.10 were found which are typical of apatite according to the ASTM standard, but from literature data it appears that under similar mineral-forming conditions the formation of hydroxylapatite is most probable. The most important reflections with intensity exceeding 0.20 were marked on the diagram. Shape of these peaks is exactly the same as obtained for the standard apatite, presented in the paper of Szpila et al. (1982). In other samples the diffractogram was reduced to the wide, diffused, asymmetric peak with maximum 2,80 Å and poorly separated reflection 3,44 Å. The two latter are the only reflections appearing when samples of poorly crystalline mass of hydroxylapatite was studied by the X — ray method. Similar pattern for poorly crystalline apatite was obtained by Szpila et al. (1982) during analysis of the kidney stone (Nr — 156.RJ).

Evidently, during chemical analysis of the hydroxylapatite-bearing sample the elevated content of calcium was found. If all amount of calcium is bonded in hydroxylapatite, about 27 wt. % of this mineral may be expected in the sample. One may calculate that about 64 wt. % of total phosphorus present in soil mass occurs as hydroxylapatite and the remainder is mostly in the decomposing organic matter taking about 1/3 of the analysed sample and in leucophosphite. Presence of the traces of this mineral was ascertained in this sample by the X — ray method.

4.3. Leucophosphite

It occurs commonly around the penguin rookery in the surficial layer of the phosphatized rocks in ornithogenic deposits. Leucophosphite is here the main identified phosphate mineral in clayey pale-yellow mass filling interstices of the rocky rubble (Tatur and Myrcha 1983). For mineralogical investigation the samples were selected with the highest content of phosphorus and the lowest amount of mineral detritus. The sample L/M was taken from the surfacial, stony soil layer on the margin of the huge rookery at Chabrier Rock (Fig. 4). The sample L/x is the clayey mass filling the interstices between cobbles of the raised beach (about 10 m above sea level). This area is on the way of the water flow-out from the biggest penguin rookery in the Admiralty Bay region near Thomas Point (Fig. 2). Pure leucophosphite was not found, but it always occurs with mineral or organic detritic material, plus other phosphates (Table III).

Powder preparation made from the leucophosphite — bearing soil material in polarized light in microscope appears to form the compact, microcrystalline aggregates of pale-yellow to light-brown color. Grains with high

Table III

Mineralogical composition of ornithogenic soils
(on the basis of X-ray analysis)

Horizons of ornithogenic soils		Sign of sample in this work	Tatur and Myrcha 1983 Profile number	Depth (cm)	Struvite	Hydroxsylapatite	8,9 A° pattern	Leucophosphite	Minyulite	Amorphous aluminum phosphate	Taranakite	Rock
		S		0—2	3	—						
			Pr 17	0—5	2	1[c]						2
	Guano	H		0—10		2		1				2
			Pr 6	0—5		2	2					2
Phosphatized rock	Surface layer	L/M		0—10		1		2	2			2
		L/x		0—10			2	2	1			2
			Pr 7	0—10			1	2	2			2
	Subsurface layer	M/x	Pr 7	10—70			2	1	2			2
			Pr 8	20—80			2	2		2[c]	2	2
		M[a]	Pr 5	60—65					3			
			Pr 5	45—70					2	1[c]		
			Pr 5	70—90					2	2		1
	Layer below ground water level	A[a]	Pr 5	90—95			1			2		1
		T[a]	Pr 6	<120							3	
			Pr. 6	<120			1				1	2

S, H, L/M, L/X, M/X, M, A, T — explanation as in Table II.
1 — trace component of the sample,
2 — important component of the sample,
3 — component of the pure monomineral sample,
a — sample after mechanical enrichment,
c — component suspected according to chemical analysis.

refractive indices (average about 1.72) in this mixture may be leucophosphite, what is in agreement with data presented by Haseman et al. (1950 b) for minerals of the group No. 4 identified by Smith and Brown (1959) as leucophosphite. This mineral is so fine-crystalline, that between crossed nicols it is almost completely isotropic. Other optic features are not discernible microscopically. In scanning microscope, auto — and hipautomorphic prisms sometimes with slightly rounded edges, densely braided and visible only under very large magnification, may be leucophosphite (Fig. 11). They occur in the finest grain classes of the analysed soils. The similar leucophosphite crystals with habit of stout prisms were described by Haseman et al. (1950 b).

Leucophosphite was identified on the basis of the X — ray reflections typical of leucophosphite and the later-described minyulite, a single very L/x. The complete pattern was obtained, characteristic both for the natural mineral (Simpson 1931-2 Lindberg 1957, Axelrod et al. 1952, Sim-

mons 1964) and for the respective synthetic substance (group 4 of Haseman et al. 1950 b). In the leucophosphite determinations performed in the above investigation, the following reflections occur most consistently: strong and very strong — 6.73 — 6.79, 5.92 — 6.08, 3.03 — 3.08: medium and weak — 7.50 — 7.61, 4.73 — 4.78, 4.20 — 4.28, 4.05 — 4.08, 3.76 — 3.80, 3.34 — 3.38, 2.95 — 2.99, 2.88 — 2.92, 2.79 — 2.83, 2.46 — 2.66. The same reflections may be found also in the diffractograms of the samples L/M and L/x, presented in the Fig. 6. In Fig. 6 the letter L marks only those specific and important reflections, which make possible the easy distinguishing of leucophosphite from the other minerals occurring in the mixture. From the comparison of the reflection intensities of the studied leucophosphite with the reflection intensities of the synthetic precipitates (Haseman 1950 b) it may be concluded that the reflections obtained for the studied sample are rather typical of the iron-potassium leucophosphite (group 4, product I) than of the iron-ammonium or aluminum-potassium phosphates, enlisted to the same group but different in some details.

The leucophosphite content certainly does not exceed 50 wt. % in the described samples, as it may be calculated from chemical analysis. Leucophosphite does not form the monomineral accumulates, but always it occurs in mixtures with other phosphates plus significant content of silicates and organic matter. Hence, the precise determination of its composition is difficult due to the above fact and its crystallochemical formula with extensive isomorphism $(K,NH_4)\ Fe^{+3},Al)_2(PO_4)_2OH \times 2H_2O$. Probably in monovalent cations the distinct prevalence of NH_4 over K should occur, and in trivalent cations Al and Fe either should be in equilibrium or Al should prevail over Fe.

In comparison with the other known occurrences of natural leucophosphite (Simpson 1931-2 Lindberg 1952, Axelrod 1952), the mineral described here is relatively poor in potassium and rich in ammonium and it contains relatively high amount of aluminum isomorphic with iron. Thus it is probably the intermediate form of leuco-phosphite similar to that described by Wilson and Bain (1976) from the adjacent Elephant Island, where natural conditions are very similar. However, leucophosphite with even higher prevalence of ammonium over potassium than that found in the present work, was described from Cave Serra do Tamandua in Minas Gerais, Brazil (Simmons 1964).

4.4. Non-identified phase with strong reflection 8,9 Å

In the diffractograms of the samples L/x and M/x besides of reflections typical of leucophosphite and the later-described minyulite, a single very strong reflection 8,9 Å was found (Fig. 6). This reflection is present also in the other samples (Table III). where it was detected together

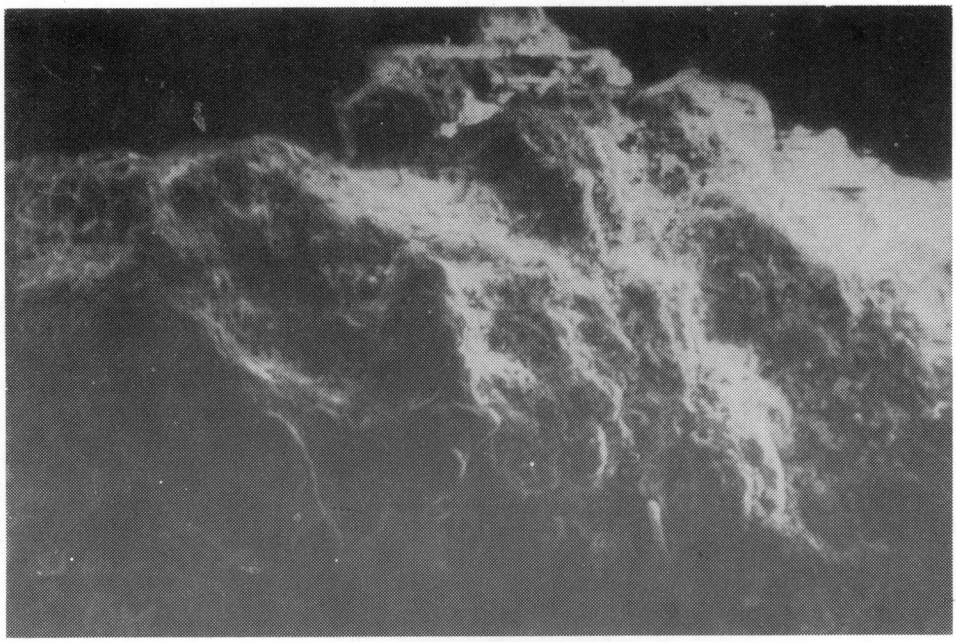

Fig. 10. Hydroxlapatite
Structure of the aggregates — irregular dripstone — type layering are visible, formed on the fine organic detritus. Scanning electron microscope image, magnification 5500x.

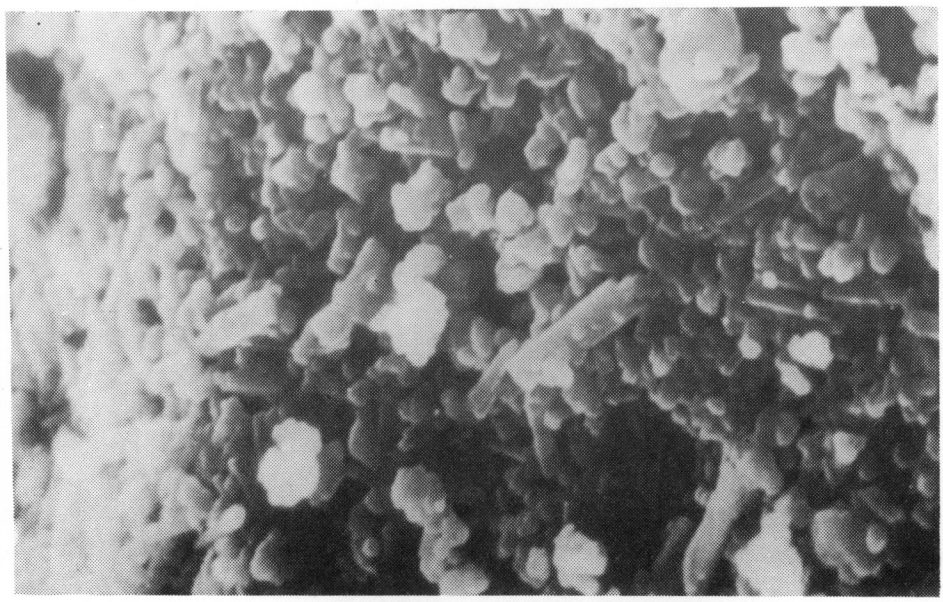

Fig. 11. Hipautomorphic prisms of leucophosphite on the background on the soil mass
Scanning electron microscope image, magnification 3400x

Photo A. Tatur, A. Barczuk

with the reflections of hydroxylapatite. Hence, this mineral form is common in the studied soils at different depths, but always it accompanies the various phosphates.

The strong reflection 8,9 Å dominating over the other reflections is pertinent to sodium-aluminum phosphate obtained by Haseman et al. (1950 a). Low sodium content in the studied sample (Table II) excludes the presence of this phosphate. Also Cole and Jackson (1950 a) obtained the synthetic phosphate with the strong reflection 8,83 Å (preparation Q). The crystal species of this preparation was formed when a colloidal iron phosphate suspension was taken to dryness on the hot plate at approximately 105 C. Chemical analyses performed from the studied samples do not exclude the possibility of presence of iron phosphates. However, in the X — ray pattern of the synthetic phosphate "Q" in addition to the very strong reflection 8,83 Å also other strong reflections occur: very strong 3,76 Å, strong 3,00 Å, medium 2,03 Å and medium 1,58 Å. Those reflections not always were found in the studied samples and even if they did, they have lower intensity. Also other iron phosphates, sodium-potassium phosphates or sodium phosphates with strong reflection neighbouring 8,9 Å (ASTM), have also accompanying reflections, not occurring in the studied samples.

For the reasons written above, the crystalline phase with strong reflection 8.9 Å still was not identified.

4.5. Minyulite

Minyulite commonly occurs in the ornithogenic soils (Table III). It is typical especially of the subsurface brown layer, where it is frequently the main phosphate mineral and it works as the cement of the clayey soil mass. Especially high concentration of minyulite was found in the profile No. 5, described by Tatur and Myrcha (1983). It is the prevailing mineral in the almost one-meter thick, phosphate hard layer of the characteristic sponge-like structure in this profile (Fig. 12). The sample M was taken from the depth 60 — 65 cm, after thorough selection of all impurities like silicates and eventual amorphous aluminum phosphate, which is a little harder and darker. Only the brittliest (easiest to ground), pale-yellow fraction of the sample material was analysed; it occupies over 70% of rock mass.

Minyulite in thin sections is visible as very fine-crystalline mass with yellow to light-brown colour and distinctly zonal structure. In aggregates of minyulite similarly to amorphous aluminium phosphate, the zonality is the irregular laminae of variable thickness, differing in the tint of the yellow-brown colour and forming spheroidal pattern that results in the botryoidal structure. The thickness of laminae ranges from 0.01 to 0.4 mm

and the thicker laminae has the lighter colour. The refractive indices of minyulite are close to the value 1.53, what is the medium refractive index for the vector β, as published for minyulite from the Adelaide area by Spencer et al. (1943). The studied minyulite contains very fine, densely packed, distinctly anisotropic scales with birefrigence difficult to the exact determination but not exceeding 0,005, which occur in almost completely isotropic mass. The determination of the other optic constans like the angle of optic axes, was not possible due to minute size of minyulite crystals.

Minyulite gives the white internal reflections in reflected light, what is the distinct difference in comparison with the frequently accompanying brown amorphous aluminum phosphate.

Sometimes around volcanic rock fragments phosphatized in various degree one may observe probably alternating, very thin rims of minyulite and somewhat thicker laminae of amorphous aluminum phosphate. Minyulite is here lighter, has higher refractive indices and distinct birefrigence in coarser-crystalline rims.

The rock formed from almost pure minyulite shows the porous structure in the scanning microscope (SEM), as in Fig. 12. The walls of pores are solid and massive with rough cleavage. They are formed from dense aggregate of very small crystals oriented perpendicularly to the pore wall surfaces. The thinning of crystals toward the massive interior of the pore walls is visible on the cleavages (Fig. 13). Surface of pores with botryoidal-spherical morphology (Fig. 14) is covered by dense druses of heads of the above-described tiny crystals (Fig. 15). Locally, under the highest obtained magnifications (about 6.000) the acicular habit of those crystals is visible. The best examples may be found in relatively rare radial (Fig. 16) or dendritic aggregates (Fig. 17).

The above-described forms of the minyulite crystallization are distinctly different than "a short prismatic habit" described by Spencer et al. (1943) from Southern Australia, but they seem to be similar to the radial aggregates of needles described earlier (Simpson and Le Mesurier, fide Palache, Berman and Frondel 1951), during the characteristics of minyulite from the Western Australia and "slender rod prisms" type of this mineral described by Haseman et al. (1950 b).

Minyulite was identified on the basis of the X — ray reflections agreeing with the natural type minyulite from Minyulo Well in Western Australia (Spencer et al. 1943). It has also the same values of main X — ray reflections as synthetic minyulite (product T group 9 of Haseman et al. 1950 b), although with some different intensities. All reflections visible in the Fig. 3, even those with the lowest intensity, belong to minyulite. The most important ones were found in both standards and the less intensive ones occur either in natural mineral or in synthetic compound.

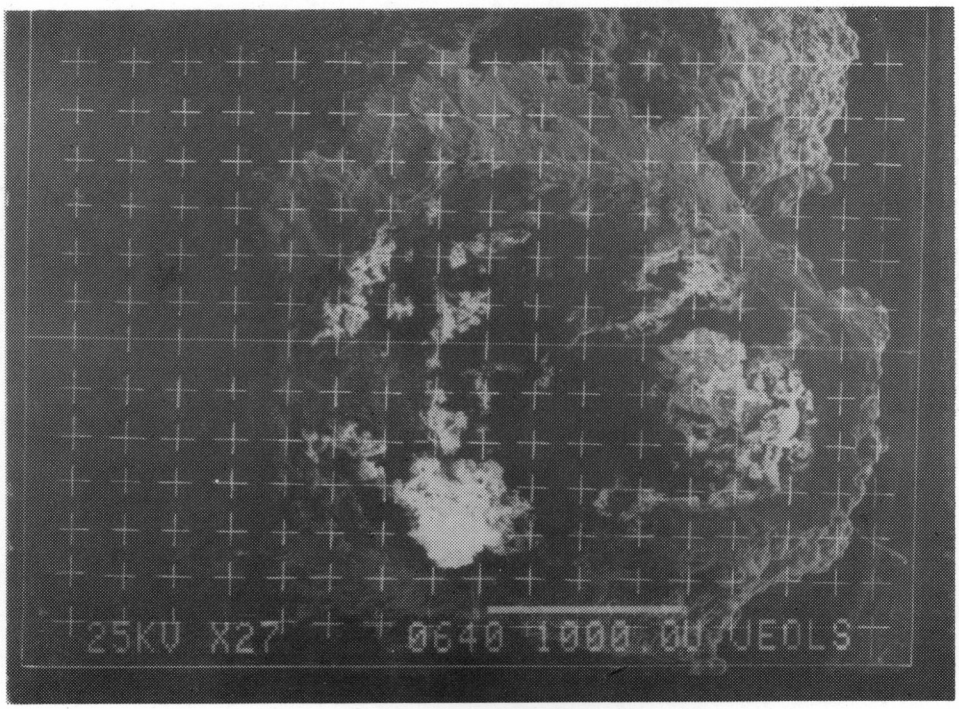

Fig. 12. The rock formed of minyulite
Porous, spongy-like structure of minyulite with traces of silica-clayey-phosphate remnants of phosphatized fragments of volcanic rocks are visible inside voids. Scanning electron microscope image, magnification 19x

Photo K. Stasiak

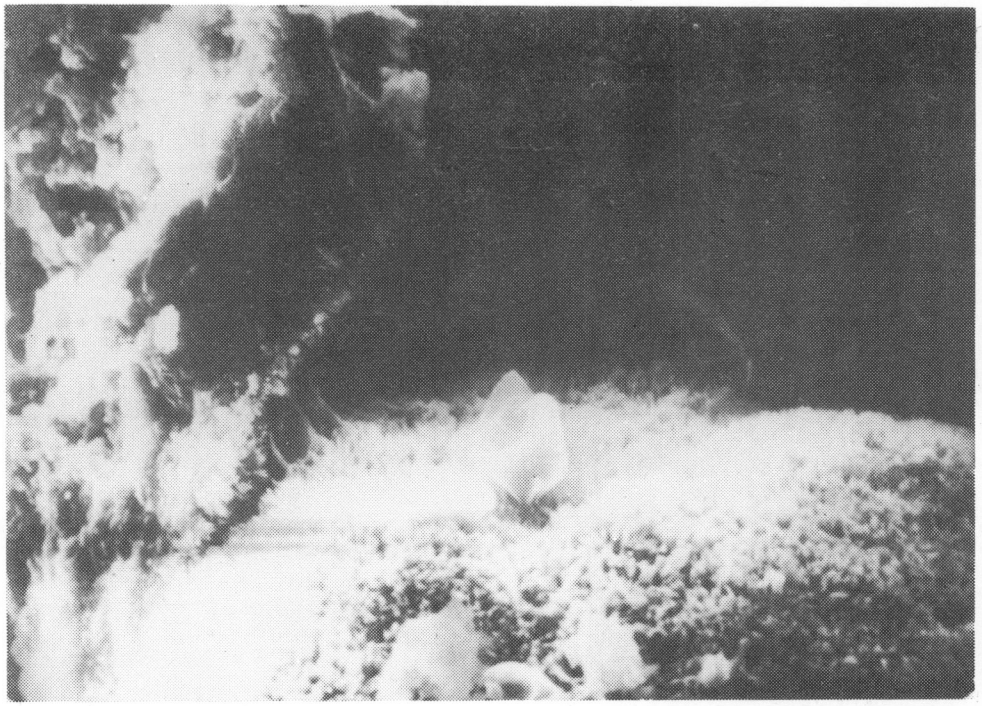

Fig. 13. Minyulite: crystal druses inside voids
Crystals grow out from the massive wall forming druses on its surfaces. Moreover, numerous not identified organic remnants are present. Scanning electron microscops image, magnification 1390x

Photo A. Tatur, A. Barczuk

Fig. 14. Minyulite. Botryoidal forms of the void interior.
Scanning electron microscope image, magnification 615x

Photo A. Tatur, A. Barczuk

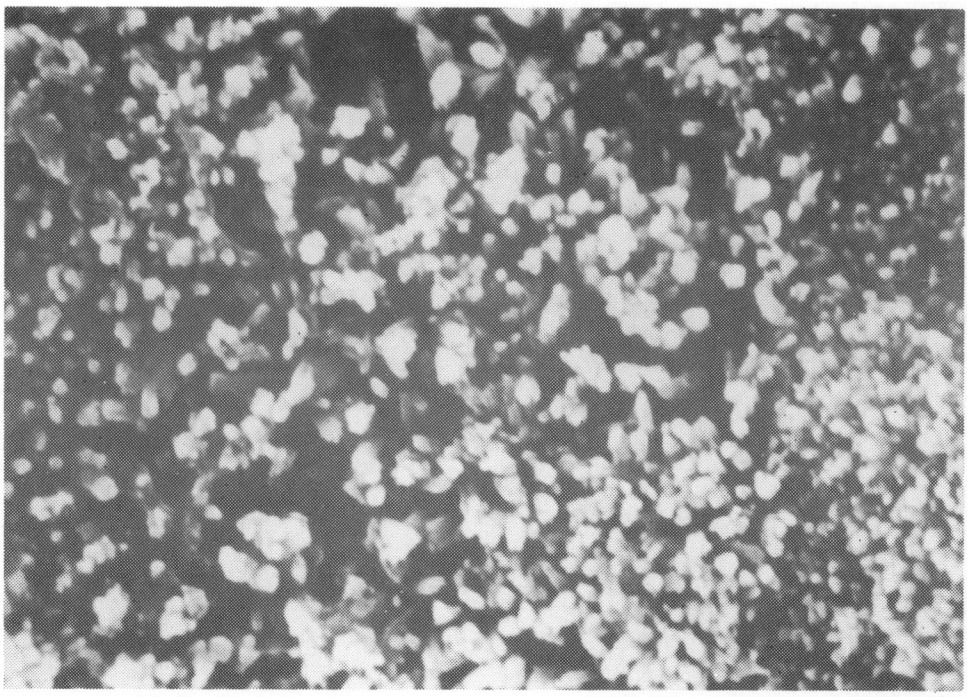

Fig. 15. Minyulite. Crystal druse covering the internal surface of void. Scanning electron microscope image, magnification 2420x

Photo A. Tatur, A. Barczuk

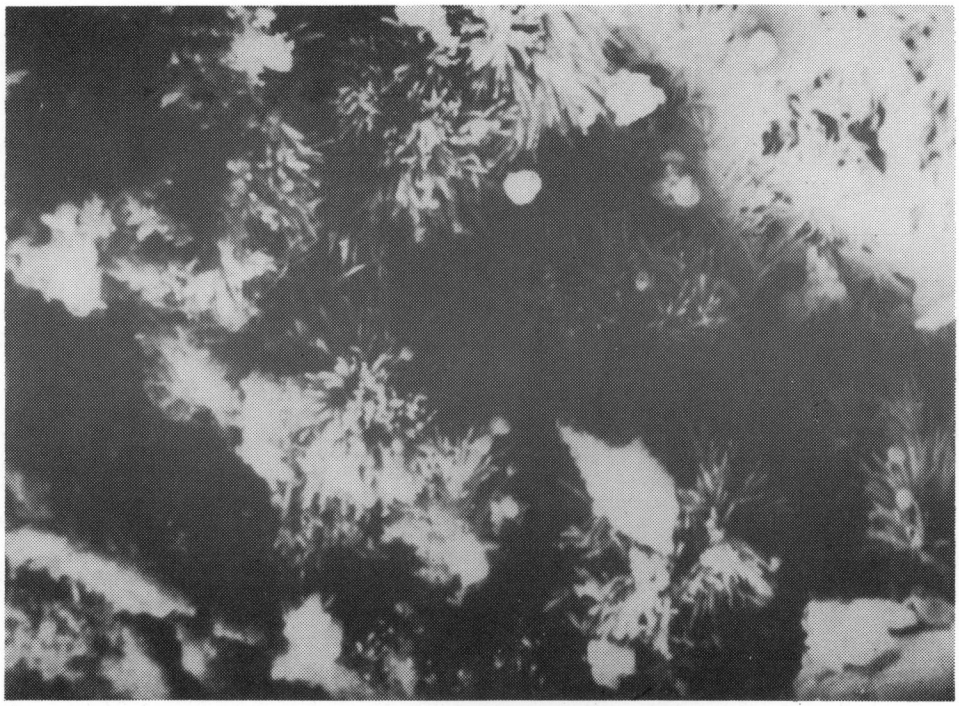

Fig. 16. Minulite. Acicular crystals forming sphereolites.
Scanning electron microscope image, magnification 1960x

Photo A. Tatur, A. Barczuk

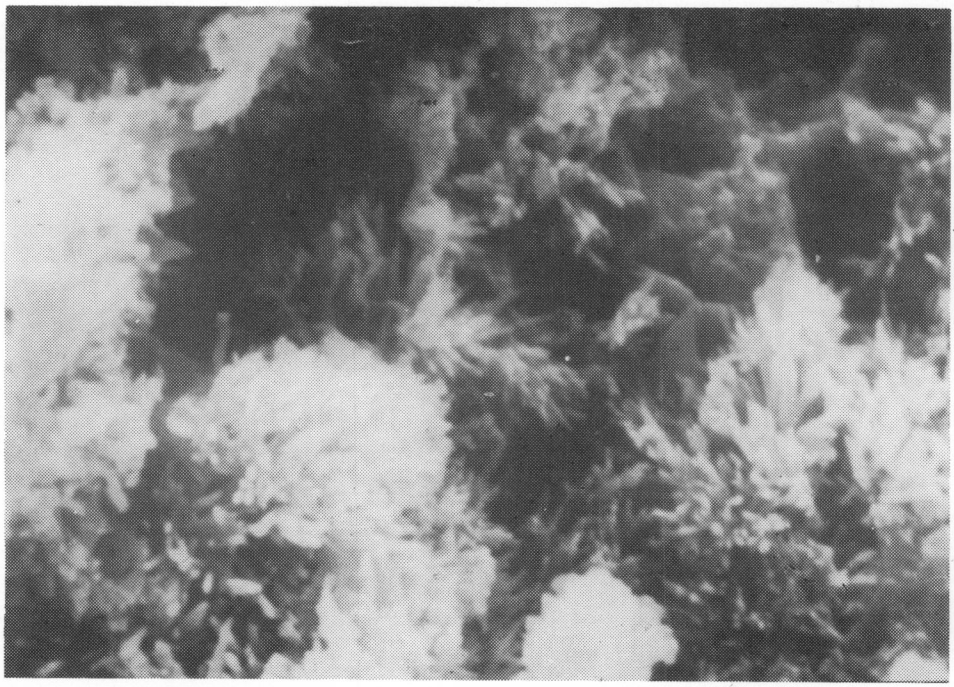

Fig. 17. Minyulite. Aciçular crystal forms concentrated in spherolitic and dendritic aggregates. Scanning electron microscope image, magnification 2650x

Photo A. Tatur, A. Barczuk

Chemical analysis presented in the Table II is the basis of calculation of the chemical formula close to the widely accepted one (Fisher 1973 a):

$$KAl_2(F,OH)\,(PO_4)_2 \times 4H_2O$$

Determinations of fluorine in the minyulite rock performed in the FRG (3.45 percent of fluorine, data owned by Prof. D. Adelung, Institut für Meereskunde, Kiel) result in completion of the above formula as follows:

$$KAl_2(F_{0.82}OH_{0.12})\,PO_4 \times 4H_2O$$

However, due to the fact that the sample for fluorine determination was not purified by mechanical way and it contained more silicate than the sample analysed in this investigation, one may suppose that fluorine content in the minyulite structure is even higher and it approaches one atom per molecule and the alternative hydroxyl group content decreases to nil. Of course this formula does not include the non-identified organic matter (C, N, H) and metals connected with the several-percent silicate admixture.

Thermal analysis of minyulite gave results more differentiated than for the other described phosphates (Fig. 7), but the absence of the literature DTA data for this mineral makes the interpretation difficult. Two distinct DTA effects at 110 and 230°C and the respective endothermic reactions recorded on the DTA curve were caused probably by the loss of hygroscopic water at the lower temperature and crystallization water at the higher one. The attempt of interpretation of the four distinct exothermic DTA peaks at 430, 480, 635 and 725°C met serious troubles. All those peaks except that at 480°C are associated with the small mass losses recorded mostly on the DTG curve. Lack of the mass loss at 480°C suggests that the reaction occurs due to recrystallization, similarly as at 630°C in taranakite. The other thermic reactions may be caused by the combustion of organic matter taking almost 10 wt. % of the sample and release of fluorine.

The numerous and various exothermic reactions may be connected eventually with the combustion of organic matter and they may be influenced by the adjacent penguin rookery and the possibility of selective bonding of groups of organic compounds by phosphates (Lewis and Scharpf 1973). Probably individual organic compounds in this environment are submitted to the specific reactions on heating, which may be the basis of their identification (Stefanovic 1957, Chesters et al. 1959). However, these possibilities do not seem applicable in this case without additional studies. At 745°C the sample melted, what was recorded on the DTA curve as endothermic reaction.

4.6. Amorphous aluminium phosphate

Amorphous aluminum phosphate forms hard, dark-brown, solid and glassy encrustations on the phosphatized detritic material of volcanic rocks. The difficulties in identification, especially in fine fractions and in mixtures with other phosphates and silicates, make impossible the unambiguous evaluation of frequency of occurrence of this mineraloid in the studied ornithogenic soils. The distinct presence of this mineraloid was detected in the profile No. 5 (Tatur and Myrcha 1983). In this profile at the depth 70—90 cm aluminum phosphate, together with the phosphatized silicate inner core, forms grains in the porous lighter and brittle mass of minyulite (Fig. 18). Deeper, at the depth 90—95 cm below soil surface, under groundwater level, after the selective dissolution of minyulite, the grains of aluminium phosphate form the layer of loose gravel. The above described aluminum phosphate after mechanical separation of other phosphates and silicate inner core, was analysed. It forms the X — ray amorphous phase (Fig. 6).

Amorphous aluminum phosphate in thin section under polarization microscope reveals the distinct zoning connected with its gradual precipitation on silicate grains. This zoning is visible in transmitted light as irregular laminae surrounding silicate grain, what results in agate-like structure (Fig. 18). Laminae of pale-yellow through brown to black colour have variable thickness, from 0.03 to 1.0 mm, and the thicker ones are lighter. Main mass of aluminum phosphate is completely isotropic, only sometimes immediately on silicate grains or next to them the light yellow, thin rims occur with low birefrigence and fibrous structure; they form microscopically different phase. Refractive index of amorphous aluminum phosphate is somewhat lower than refractive index of Canada balsam, ranging from 1.46 to 1.48. This value is close to the data presented by Taylor and Gurney (1960). Refractive index of the birefrigent phase is distinctly higher than that of amorphous aluminum phosphate or Canada balsam. But refractive index of the coexisting minyulite is higher than refractive index of amorphous aluminum phosphate but a little lower than that index of Canada balsam.

Phase with initial birefrigence present in amorphous aluminum phosphate has light yellow colour and fibrous structure (fibers are perpendicular to the surface of silicate grains). Birefrigence ranges from about 0.01 to 0.015 and its value depends probably either on the various degree of crystallinity or on the variaton of chemical composition.

Amorphous aluminum phosphate in the scanning microscope shows the massive structure, best visible on the cleavage surface (Fig. 19). Such surfaces are relatively flat, rough and matt. In pores, voids and on external surfaces where minerals might crystallize freely, the botryoidal aggregates with smooth surface formed due to dripping-water activity (Figs. 19 and 20). Locally the irregular accumulates of rounded plates are discernible with use of

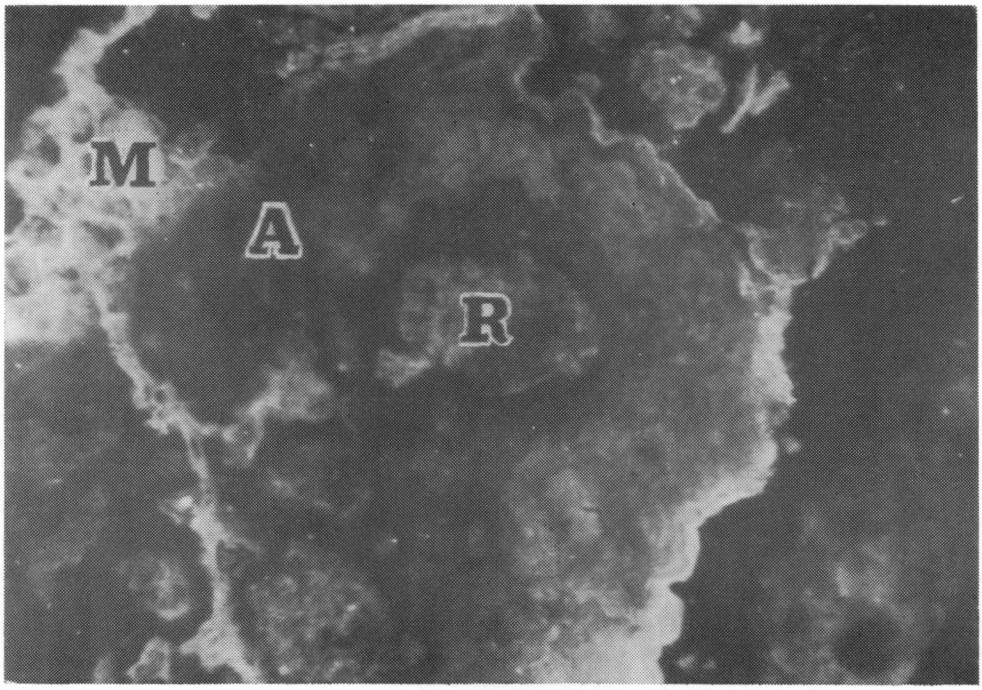

Fig. 18. Amorphous aluminum phosphate with agate-like structure
(A) — amorphous aluminum phosphate surrouding the fragment of the phosphatized volcanic rock (R). Outer layer cementing individual grains consists of the brittle minyulite mass (M). Polished section, reflected light image in the polarization microscope, magnification 65x

Photo A. Tatur

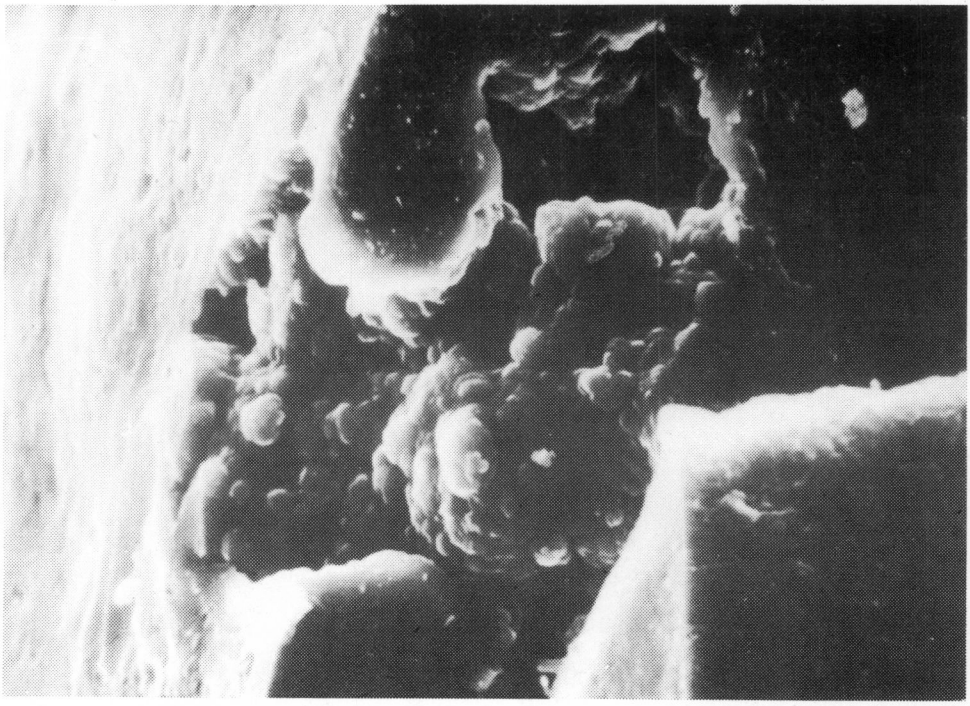

Fig. 19. Amorphous aluminium phosphate. Dripstone-type surfaces of precipitation. Scanning electron microscope image, magnification 780x

Photo A. Tatur, A. Barczuk

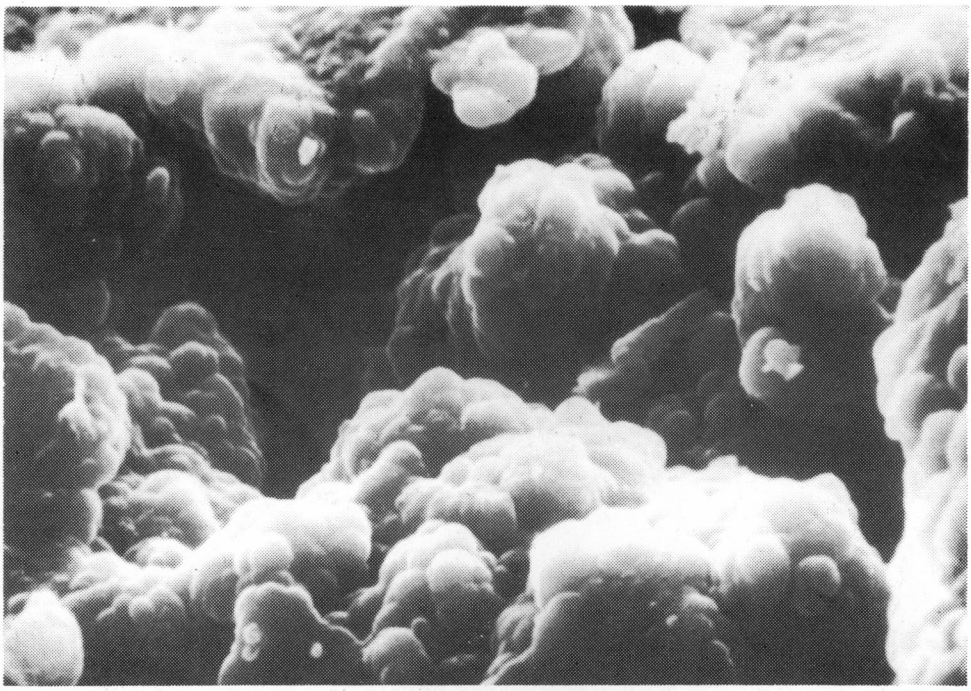

Fig. 20. Amorphous aluminium phosphate. Boryoidal dripstone type surfaces of precipitation. Scanning electron microscope image, magnification 2110x

Photo A. Tatur. A. Barczuk

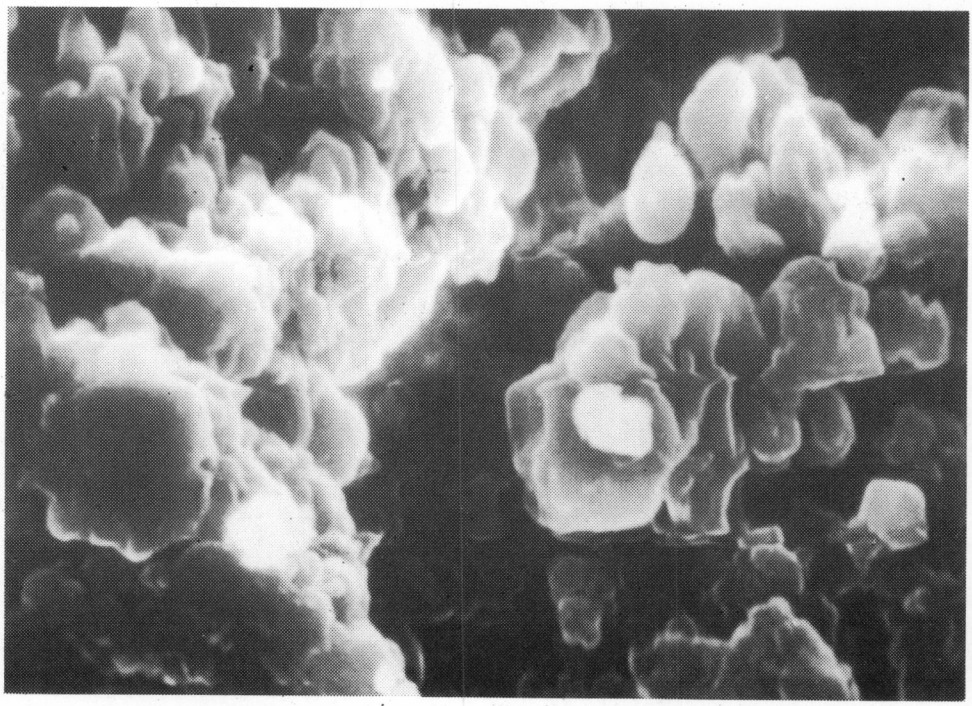

Fig. 21. Variscite-like forms in amorphous aluminum phosphate
Rounded flakes are arranged in layers. Scanning electron microscope, magnification 4170x

Photo A. Tatur, A. Barczuk

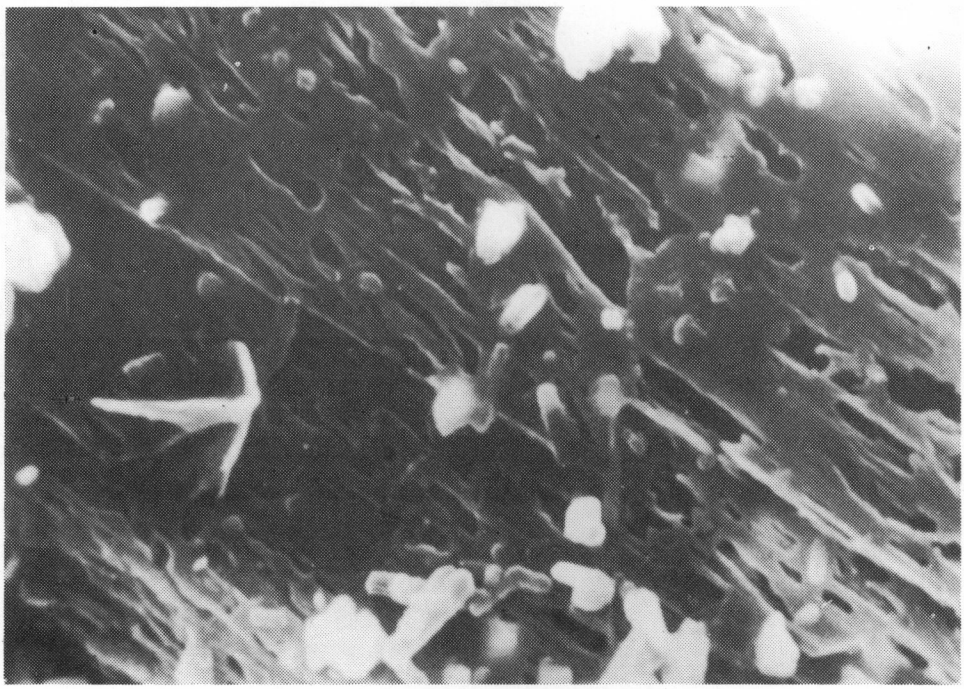

Fig. 22. Amorphous aluminium phosphate. Open-work corrosion structure. Scanning electron microscope image, magnification 3240x

Photo A. Tatur, A. Barczuk

high magnification. Such accumulates may be on initial stage of variscite crystallization (Fig. 21) and they tentatively are compared with the low-birefrigence phase visible under polarization microscope. Similar crystal habits of variscite were found by Haseman et al. (1951).

The nature and chemical composition of amorphous to X-ray mineraloid seems to be similar to the one described earlier as vashegyite (massive amorphous vashegyite in paper by Koch and Sarudi 1963). However, according to data given by Koch and Sarudi (1963), possibility of formation of crystalline vashegyite from amorphous one, should also not to be excluded. Crystalline vashegyite was described also in comparable conditions in parągenesis with taranakite on the shore of New Zealand Island (Bannister and Hutchinson 1947).

In the sample from the profile 5, depth 90—95 cm, the distinct corrosion forms were found as regular elongated depressions distributed paralelly (Fig. 22).

The approximate formula of the studied aluminium phosphate $AlPO_4 \times \times 5H_2O$ may be derived from the chemical analysis (Table II). Small prevalence of Al over P is caused rather by some clay material that contamined the sample during mechanic separation than by nature of this compound.

High content of strontium is apparent among the subordinate elements probably due to the selective absorption from the flowing groundwater. This strontium is believed to be of ornithogenic origin (Sr content in krill ash is 0.17 wt.%, Tatur and Myrcha 1984) next released during mineralization of the organic matter. The ability of the selective concentration of strontium is the feature of numerous phosphate minerals (Altschuler 1973, Frondel, Ito and Montgomery 1968). This phenomenon used to be explained by the rules of isomorphic replacement of calcium and potassium by strontium as in crandallite (Frondel 1958). However, in the studied case, a different explanation should be proposed.

Very high hydratation of this mineraloid was also stated during performing of chemical analysis. It is the highest in the studied phosphate group and over two times higher than in crystalline variscite. Results of DTA prove that dehydration starts clearly below 100°C but the stages of dehydration typical od crystalline phosphates were not observed (Fig. 7). Maximum of the dehydration endothermic reaction (165°C) occurs at lower temperature than for taranakite and minyulite. The double exothermic reaction at 520°C (smaller peak) to 550°C (greater peak) is similar to the double peaks occurring at different temperatures for minyulite (430, 480°C) and taranakite (590, 630°C). The difference between the two minerals and the studied mineraloid is that the main peak here is associated with the noticeable mass loss, what suggests the connection of this peak with combustion of organic matter. This phosphate bears more organic compounds

than other phosphates, i.e., about 10 wt.%. The absence of the other exothermic reactions characteristic for overlying minyulite layer may prove the distinct selection of organic compound sorption by various phosphate minerals and/or mineraloids.

4.7. Taranakite

Taranakite was found in the deeper, always humid soil layers. It may occur in paragenesis with other phosphates (Table III) as well as it may form monomineral accumulations. Pure taranakite was found in the profile No. 6 (Tatur and Myrcha 1984) at the depth below 120 cm (Fig. 3). It looks like white clay filling the interstices between boulders and smaller phosphatized rock fragments. Taranakite occurs in a layer below the ground water level. Due to presence of taranakite in the bottom of the rocky soils, its real distribution is difficult to evaluation.

In the microscope preparation made from the dry taranakite powder immersed in Canada balsam the cryptocrystalline structure was revealed. Individual, either very fine (average dia. about 0.02 mm) or sometimes submicroscopic flaky crystals generally are sub-paralelly oriented. Locally slightly undulated flakes reach 0.3 mm in length. They have light-green colour and birefrigence 0.01—0.013, whereas the surrounding fine-grain taranakite mass is colourless and with low interference colours or it is almost completely isotropic. These features probably are due to the very minute crystal size of main taranakite mass. Refractive indices of this mineral measured in the mass as average value of the various crystallographic directions, are equal to about 1,50 what does not differ from the data presented by Haseman et al. (1950 b). Other optic features of taranakite were not measured because of too small crystal size.

In scanning electron microscope (SEM) taranakite was visible as compact clay of generally parallel hexagonal plates of almost automorphic habit (Figs. 23 and 24). Habit of hexagonal plates (Fig. 25) is typical of this mineral (Haseman et al. 1950 a, b).

Taranakite was identified on the basis of the X — ray studies, since the obtained X — ray powder pattern is in agreement with the pattern of the natural standard mineral from the shore of New Zealand (Bannister and Hutchinson 1947). In details the obtained data are very close to the newer, more exact diffractograms (Murray and Dietrich 1956) and synthetic (Haseman 1950 b) taranakites, both ammonium and potassium varieties (Arlidge 1963).

Chemical analysis showed that taranakite from King George Island has a little higher P:Al ration than the other natural taranakites (Bannister and Hutchinson 1947, Murray and Dietrich 1956). This feature

makes it similar to the standard synthetic taranakite (Haseman 1950 b). For this reason, despite the numerous published crystallochemical formulae, the formula proposed by Fisher (1973) is most appropriate for the studied taranakite. Hence, the crystallochemical formula of this mineral from the King George Island may be written as follows:

$$K_{1.9}(NH_4)_{1.1}Al_5H_6(PO_4)_8 \times 18H_20$$

This formula includes neither elements present in the non-identified organic compounds (C, H, N) nor some admixture of elements attributable to clayey fraction (iron, insoluble part) and certain excess of water. Thus the determined taranakite is, like the other natural ones (Bannister and Hutchinson 1947, Murray and Dietrich 1956), an intermediate potassium-ammonium variety. The isomorphic substitution of aluminum by iron is insignificant or even absent, being in agreement with the Arlidge's (1963) conclusions.

Certain crystallochemical features of the studied taranakite were distinctly discernible in thermal analysis (Fig. 7). Three-stage mass loss at temperature 140, 160 and 180°C visible only on the DTG curve, and associated with the weakly splitted (160 and 190°C) endothermic effect, corresponds to the dehydration of taranakite and its alternation probably through the known

Table IV.

Comparison of X-ray powder pattern of vivianite from King George Island with the data presented by Vasilev et al. (1974)

Vivianite from King George Island		Data after Vasilev et al. (1974)	
d/n Å	Intensivity	d/n Å	Intensivity I/Io
8.00	W	8	27
6.80	VS	6.80	100
4.80	M	4.81	40
4.60	W	4.50	13
4.08	W	4.09	13
3.84	M	3.84	40
3.63	VW	3.65	5
3.34	VW	3.35	3
3.20	S	3.20	53
2.97	S	2.97	67
2.71	S	2.71	67
2.52	M	2.52	33
2.43	M	2.42	40

VS — very strong
S — strong
M — middle
W — weak
VW — very weak

lower hydrate phases to the product amorphous to X — ray finally (Murray and Dietrich 1956). The above-cited authors found on the basis of DTA curve the two stage dehydration of natural taranakite from Pig Hole Cave, and Arlidge (1963) also from the DTA concluded the one stage dehydration of synthetic taranakite.

The mass loss at temperature from about 200°C to almost 400°C distinctly visible on the DTG curve and corresponding to the weakly recorded on the DTA curve endothermic reaction, most probably is connected with the release and evaporation of ammonia. Arlidge (1963) has gotten the similar effect on the DTG curve of synthetic ammonium taranakite.

Due to the absence of good data one may not elucidate unambiguously the reason of the appearance of the splitted exothermic effect marked on the DTA curve at temperatures 590 and 630°C. Exothermic reaction between 500 and 600°C, typical exclusively of the potassium taranakites and not associated with any mass changes, after Arlidge (1963) is due most probably to a recrystallization.

Thus, probably the respective exothermic reaction was recorded for the studied taranakite at somewhat higher temperature, but the splitting of peak is still an enigma. Endothermic reaction at 835°C is connected with melting of the sample.

4.8. Vivianite

Vivianite was found in clay underlying peat at the depth of 0,5—1,5 m in the marginal zone of the probable interaction of solutions flowing out from the penguin rookery. Because in other places out of the penguin vital activity area vivianite was not found it is very probably that this mineral in the discussed location should be of ornithogenic genesis. It occurs as unstable blue aggregates in gray clayey mass and frequently it forms the thin layer covering pebble. From this layer the sample was taken. Due to scarce amount of the collected material, the identification was made by the X — ray method of Debye-Scherrer-Hull. The obtained powder pattern is typical of the standard vivianite (Table IV). No admixture of the other crystalline substances was found.

4.9. Krill

In the dried and ground krill the only mineral giving distinct X — ray reflections in the background of amorphous organic matter is halite. Halite presence appears also unambiguously from chemical analysis and proves

the high content of sea water in the food carried by penguins on the land. Trace amounts of halite also used to be detected in the surface layer of the ornithogenic soils in the rookery area.

4.10. Mineral composition of the ornithogenic soils

In the studied ornithogenic soils the monomineral phosphate mass accumulates only locally. Usually in the fine grain of the soils there were found two or three phosphates mixed with silicates and organic matter (Table III). Minerals connected with the surface guano layer mix in low degree with minerals occurring in the underlying zone of the phosphatized rocks. However, in the zone of the phosphatized rocks almost all possible combinations of minerals parageneses were found. In the studied samples only simultaneous occurrence of minyulite and taranakite was not stated, but it may be accidental due to small number of samples. One may not conclude that those two minerals occur alternatively.

Despite the monotonous chemical composition of the phosphatized rock zone (Tatur and Myrcha 1983), the mineral analysis explains the visually recognizable differentiation of soils in the genetic levels.

The soft, light yellow mass of loamy aggregates in subsurface horizon of the soil subsurface clayey soil mass occurring between rock rubble bears usually leucophosphite as the prevailing mineral.

Minyulite is commonly the main mineral of the deeper subsurface layer, consolidated and darker. Sometimes amorphous aluminum phosphate takes place of minyulite, especially in the bottom part of this layer.

Amorphous aluminium phosphate or taranakite concentrate in the deepest layer below the ground water level.

5. Discussion

The vertical sequence in the distribution of the phosphate minerals occurs in guano and the underlaying silicate weathering crust phosphatized by guano leachates. The sequence from the Earth's surface downward is as follows. Struvite occurs only on the soil surface, hydroxylapatite in the whole surface guano layer, leucophosphite is typical of the most shallow, subsurface zone of phosphatized rocks. Minyulite is commonly the prevailing mineral in the deeper layer, where it may occur in paragenesis with amorphous aluminium phosphate especially in the bottom part of this layer. Domination of taranakite was found in the deepest levels.

The distinguished sequence of phosphate minerals forms either as precipitate from solutions or as the product of the metasomatic reactions between

water solution and soild phase of soil. Differentation of the formed minerals and their vertical distribution have to be in a distinct connection with chemical composition of water solutions percolating through soils.

Chemical composition of the nutrient-rich ornithogenic water, dynamically self-altering during infiltration through the ornithogenic soils was analysed in details in the paper by Tatur and Myrcha 1983 b). Table I presents also the selected analyses from this paper in addition to the analyses of waters characterizing the environment of origin of the studied phosphates. Those data help to recognize the ranges of water metamorphosis already after a few-matter percolation through the ornithogenic soil during several days.

Waters running off from the penguin rookery on the soil surface are alkaline or neutral with variable, frequently very high concentrations of mineral phosphorus and nitrogen and with the distanct domination of ammonium over nitrate form of nitrogen compounds. After percolation through soil the chemical composition is stabilized and reaction becomes acid (pH 4 or insignificantly higher). Nitrate nitrogen dominates over ammonium form. The above-described metamorphosis of chemical composition of waters occurs due to volatilization to atmosphere, sorption, bounding in crystal structures of phosphates and nitrification of the alkalizing ammonium. The number of autotrophic nitrifying bacteria was increased from 80—100 cells per 1 g of the soil in organic surface horizons to 460—750 cells per 1 g of soil in lower horizons (Pietr in prep.). Also mineralization of organic matter with secretion of oxalic acid supports the acid reaction of waters. Definitely, the acid reaction of waters is stabilized as the result of their reaction with phosphates present in the bottom of the ornithogenic soils.

Experimental data (Cole and Jackson 1950 b) suggest that paragenesis of minyulite plus variscite during stabilization of the solubility equilibrium constans by the buffering phase changes, causes the pH value of solution equal about 4. Close to that pH value is typical of all analysed water in the area under study if they percolated earlier through the phosphatized weathering crusts (Tatur and Myrcha 1983 b).

The above disccused-variation of pH of solution infiltrating through ornithogenic soils seems to be simpliest factor influencing the vertical changes of mineral composition in the profile of the studied soils. It is commonly known that hydroxylapatite, the main mineral of the analysed guano, may form and exist only in alkaline or neutral environment, where it is also the least soluble of the several calcium phosphates under neutral conditions, but it becomes more soluble in acid solution (Brown 1973). Seemingly, the decrease solely of pH value of guano leachates during percolation through the soil in the presence of aluminium and iron ions, may cause the supersaturation of solution with respect to phosphate ions and precipitation of phosphates (Stumm and Morgan 1970). Leucophosphite occurring in

the subsurface layers forms as precipitate from neutral or weakly acid solutions (pH from 7 to 5), but taranakite, which occurs deeper, from acid and strong acid solutions (pH from 5.3 to 1.7) (Haseman et al. 1950 b). Positions of minyulite and amorphous aluminium phosphate in the vertical soil profile suggest that those minerals originate from solutions of the intermediate pH values. This genetic feature is not excluded in papers discussing the origin conditions of those minerals, but such conclusion is not evident (Haseman et al. 1950 b, Cole and Jackson 1950 b, Hsu 1982). The connection of genesis of the discussed mineral sequence only with the changing pH without evaluation of the other influence, however, would be a reckless and simplified supposition.

The laboratory studies and field examples result in conclusion that the domination of aluminium-iron phosphates containing and ammonium observed in the zone of the phosphatized silicate weathering crusts is connected generally with the alkali excess in solutions and leucophosphite, minyulite and taranakite are minerals that form initially under such conditions (Altschuler 1973).

Preference of formation of the defined mineral form this group is in some connection with pH of the parent solution (see above). However, the exact conditions preferring origin minyulite than leucophosphite as well as taranakite, are not known (Taylor, Gurney and Lindsay 1960). At least in some range the pH values necessary for synthesis of those minerals overlap one another. The occurrence of paragenesis of leucophosphite plus taranakite without intermediate minyulite (Table III) was ascertained, what would be rather improbable if the changing pH value is the only factor controlling the origin of those minerals.

The collected petrographic material suggests that minyulite forms usually hard coat overgrowing the weathering rock fragments, probably bounding aluminium released from those fragments. Unlike leucophosphite and taranakite which are clearly the products of precipitation from solutions, minyulite forms almost *in situ* in the process of metasomatic phosphatization. Probably the significant role is displayed by high concentration of ornithogenic salts, occurring especially in the immediate neighbourhood of the penguin rookery, where this largest accumulation of minyulite was found. It seems also that fluorine is especially important ornithogenic element, maybe even conditioning the origin of minyulite. Fluorine is present in the structure of this mineral, what was showed by Spencer et al. (1943) for natural minyulite. The presence of fluorine is necessary also during synthesis of this mineral (Haseman 1950 b). Content of 3,45% F in minyulite from the King George Island (Adelung, personal communication) proves that minyulite is one from the most important minerals eliminating fluorine from the biogeochemical cycle caused by the penguin vital activity. The determined concentration of fluorine (0.82 atom per molecule) is even

higher than in the described (Spencer 1943) minyulite from Australia (0,5 atom per molecule). This amount approaches the fluorine content in synthetic minyulite (Haseman 1950 b), equal 1,0 atom per molecule. The latter author obtained it submitting very high fluorine concentration in parent solution on the precipitate. Probably minyulite may form exclusively around rookeries of birds feeding with food of high fluorine content. Probably for this reason minyulite was not found around rookeries of the fish-eating birds, presently most frequently studied, but is was recognized near the rookery of the krill-eating penguins. Fluorine content in krill is higher than average, and in fish it is much lower and equals (Soszka et al. in prep.).

The common occurrence of the ammonium ion on the soil surface may be the factor favourable for leucoposphite formation. In this mineral the isomorphic replacement of potassium by ammonium seems to be common, but in the deeper-seated minyulite, even if it occurs, it concerns very small part of potassium.

Among the identified phosphates of the zone of phosphatized rocks, only leucophosphite bears in its structure significant amount of trivalent iron. The existence of trivalent iron is possible mostly in the periodically dried and thus better oxygen-saturated surface soil layer. This is one more way of explanation of more frequent occurrence of leucophosphite in the surface layer. Continuous humidity of deeper levels plus presence of significant amount of organic compounds coming from guano decomposition favours the iron reduction to bivalent form, not bonded in the mineral structure but easily washed out from soils and resulting this way in promotion of the formation of aluminium phosphate instead of iron phosphate (Hsu and Jackson 1960).

The last of the group of the discussed aluminium-iron phosphates bearing potassium and ammonia — taranakite, forms as precipitate in the deepest always humid soil layers, where solutions are most acid and most diluted. Its occurrence seems to be typical of zones of stagnation of alkali-rich ornithogenic waters. Significant dilution may be also important condition of origin of this mineral as the above-discussed low pH value. Haseman et al. (1950 b) also obtained the described synthetic tarankites from more dilute solutions than leucophosphite and minyulite. However, those authors in numerous experiments did not find the connection between salt concentration in solutions and phase composition of the forming precipitate.

Leucophosphite, minyulite and taranakite form in the presence of excess alkali, but if solutions are poor in alkali or if aluminium and phosphate ion activities are sufficiently high, one should expect the origin of simple aluminium phosphates either precipitating immediately from solutions (Hsu 1982), or forming due to incongruent dissolving of minyulite (Cole and Jackson 1950 b) or taranakite (Taylor and Gurney 1961).

The paragenesis of amorphous aluminium phosphate plus minyulite in the studied ornithogenic soils and it has been described in details (Tatur and Myrcha 1983, profile No. 5). In the upper part of the phosphatized rock zone (depth 15—70 cm) minyulite distinctly prevails. Presence of certain small amount of amorphous aluminium phosphate seems to be suggested by microscope observations. Thin laminae in minyulite encrustations may be this mineraloid here, since they have distinctly higher refractive index. Also mole ratios between potassium, aluminium and phosphorus (Tatur and Myrcha 1983 a) would indicate the presence of up to 30% aluminium phosphate, if minyulite occurring in the analysed samples occurs as pure aluminium-potassium phosphate, without isomorphic replacement of potassium by ammonium. Hitherto investigated minyulite specimens (Spencer et al. 1943, Haseman et al. 1950 b) and that described in this paper are potassium varieties exclusively.

In the deeper part of the profile, amorphous aluminium phosphate becomes dominating phase. Its unambiguous identification was possible here due to use of X-ray analysis. At the depth 70—90 cm in light-yellow porous mass of minyulite, the hard grains of sandy and gravel fraction occur, formed by dark brown hard coat of encrustations of amorphous aluminium phosphate on phosphatized rock fragments. Those grains after selective dissolution of minyulite by mobile ground water, form loose gravel in the bottom of profile No. 5 (90—95 cm.)

It is difficult to conclude unambiguously if the desribed amorphous aluminium phosphate occurs due to immediate precipitation from solution or as a product of alteration of the earlier formed minyulite. Overgrowing surfaces observed in amorphous aluminium phosphate in the scanning microscope (Figs. 19 and 20), also in the variscite-like variety (Fig. 21), which are different than growth surfaces of minyulite (Figs. 13 and 14) suggest at least in this case the possibility of immediate origin of this mineraloid by this way that aluminium ions released from soild phase, precipitate from soil solutions phosphate ions, always occurring in excess.

However, on the other hand, the contact between those phases observed in thin sections (Fig. 18) suggest that amorphous aluminium phosphate grows due to incongruent dissolution of very thin minyulite layers overgrowing it. Such alterations might be caused by aluminium ion released from silicates decomposing in the inner core of the grain. Also repeating wash-out of soils by waters with high and next low total mineralization may cause such alteration. Minyulite formation would occur during percolation of guano leachates through soils after summer rainfalls, and incongruent dissolution would develop in the rain-free periods when the rookery area is dry and weakly mineralized waters are submitted by melting snow and soil permafrost located below the rookery. Acceptance of the latter hypothesis would explain also genesis of thin layers of amorphous aluminium phosphate observed

inside minyulite shellings in the upper part of the phosphatized zones. They may form during the periodic washing of minyulite by weakly mineralized waters. Such observation confirms the anticipation of Taylor and Gurney (1961). Those authors thought that formation of thin layer of amorphous aluminum phosphate on the surface of incongruently dissolving minyulite significantly protects this mineral from the further alteration, what explains the progressive delay of those dissolution.

It is possible that amorphous aluminum phosphate forms by several different ways, depending on the locally and periodically changing physico-chemical conditions. On the basis of Larsen's experiment (after Palache, Berman and Frondel 1951) made with variscite, the possibility of reverse reaction should be also accepted i.e. the alteration of simple amorphous phosphate in the composite aluminium -potassium or aluminum-calcium phosphates. Such reaction may occur due to high calcium and potassium concentration in solutions.

Microscope observations show also that genesis of this mineraloid like genesis of minyulite, generally is connected with metasomatic processes. No need to suppose the ionic transport of aluminum in solutions for explanation of its genesis.

During the detailed investigations of thin sections in the polarized light, amorphous aluminum phosphate appeared to be the optically nonhomogeneous phase. In the layered structure of this mineraloid, there occur laminae with distinct birefrigence. Especially frequently such laminae were found on the phosphatized rock fragments. Optical features of this phase exclude the common occurence in the neighbourhood of minyulite, but they seem to indicate variscite. Also in the scanning microscope in some places of amorphous aluminum phosphate one may observe the variscite-like structures. The above features suggest the possibility of variscite presence of rather initial stage of its crystallization, since the X — ray analysis did not reveal any trace of crystal phase. Absence of crystal phase in the X — ray record may be caused both by poorly crystalline material and by small amount of crystal phase in the studied sample (few percent only).

Relatively detailed analysis of formation conditions of variscite and amorphous aluminum phosphate was performed by Hsu (1982). According to data obtained by this author, variscite formation instead of amorphous aluminum phosphate is promoted by pH decrease below the value 4. Product of precipitation from solution at pH 3.3 (and sufficiently high concentration of aluminum and phosphorus in solution) consisted of 20% variscite and 80% amorphous aluminium phosphate after 45 months of aging, but at pH 4 and higher, amorphous aluminum phosphate was obtained, initially with mole ratio P/Al distinctly higher than one (1.23—1.35), and after further aging for one year it altered in the phase with P/AL ratio close to one (0.96—0.96). Amorphous aluminum phosphate with P/Al ratio

0.91 found in the studied soils, seemingly represents the final phase after selective removal of the phosphorus excess over aluminum probably existing in the fresh precipitate; such removal may be due to incongruent dissolution. At pH 1.0, 2.6 and 2.9 variscite was finally obtained.

In the studied soils the promoting conditions for variscite formation might appear in short periods when pH of ornithogenic waters supposedly decreased below 4 (e.g. due to nitrification), and buffering phase reactions did not elevate it to the final value 4 in this system (Cole and Jackson 1950 b). Also it is possible that like in Hsu (1982) experiment also here crystallization of variscite passed through an unidentified aluminum hydrogen phosphate as intermediate compound.

Struvite position in the sequence describing the dependence of genesis on the pH value only, also doesn't seem to be sufficiently evident. Experimentally struvite has been obtained in large crystals by slow reaction of magnesium sulfate solution with acid solution of ammonium phosphate (Palache, Berman and Frondel 1951). In the studied area the highly ammoniacal conditions necessary for origin of this mineral (Hutchinson 1950) occur only in alkaline surface waters.

It is commonly known that the factor conditioning the origin of struvite is also magnesium presence in solutions (Hutchinson 1950). Magnesium may come from the weathering underlying rocks, from sea water carried on the land in aerosol by wind or transported by penguins with food. Importance of the latter way was presented in the paper by Tatur and Myrcha (1963). Sodium content in water is strongly correlated with the nutrient amount and it is distinctly higher in waters flowing out of the rookery area than in the surrounding area. This feature was confirmed by the X — ray analysis (Fig. 6) and chemical determination (Table II) revealing the high content of sea salt in the fresh krill eaten by penguins. It is possible that specific chemical features of ornithogenic waters from which the studied struvite crystallized, are the reason of characteristic crystal habit, different than the described earlier (Palache, Berman and Frondel 1951).

Physico-chemical conditions necessary to formation of the unidentified crystalline phase with strong reflection 8.9 Å are also difficult for deduction. This phase has been met mostly in paragenesis with leucophosphite, but it may exist as well in guano with hydroxylapatite or in the phosphatized silicate fragments in the taranakite clay. Thus it is phase with the widest range of occurence and the weakest inclination for formation of monomineral agglomeration.

Vivianite problem should be discussed individually. Vivianite occurs out of the zone of ornithogenic soils in continuously humid clay layer under less than one meter thick peat layer. This level bears organic matter of distinctly plant origin. Humus content is about 5 wt.% and C/N ratio is equal to about 12. The described location may be periodically under limited influence of

ornithogenic waters which are the quite probably source of phosphorus for widespread here vivianite. Vivianite occurs as variety of deep blue color, characteristic for locations (also in our climatic zone) in the swamp areas with limited oxygen amount.

In the mineral composition of the described ornithogenic soils, the phosphates geologically unstable are mostly present, especially in the Maritime Antarctic Zone with its high annual rainfalls. The persistence of these phosphates is due to the continuous manuring supporting the specific physico-chemical conditions in the neighbourhood. Longer break in manuring has to cause the trend, common in this zone to soil acidification. In connection with washing of the soils by weakly mineralized atmospheric waters, the above discussed factors should cause first the dissolution of minerals occurring in guano: struvite and apatite (Hsu and Jackson 1980, Van Wazer 1961). Also dissolution of potassium- and ammonium-bearing aluminum-iron phosphates should be anticipated, which although are more stable in acid medium (Hsu and Jackson 1960), become unstable in solution poor in alkalis (i.e. weakly mineralized). Amorphous aluminum phosphate would be most surely the product of their incongruent dissolution under the studied conditions, if it has not enough time to dissolve (Fig. 22). In this case, in the aging process this amorphous aluminum phosphate may only recrystallize to variscite or eventually vasheqyite. Variscite which was probably found also in the studied samples, has higher stability in acid soil media (Kittrick and Jackson 1955, Taylor and Gurney 1962, Taylor 1963, Hsu 1982), but it also dissolves with the rate depending on the pH value (Bache 1963). However, in the light of the experiments performed by Hsu (1982), crystallization of amorphous aluminum phosphate in variscite does not seem likely, at least during one-year observation.

In the discussed ornithogenic soils the mineral system was observed which is the result of unstable equilibria between opposed processes. The first is the formation and maintaining of persistence of formed minerals due to continuous manuring. The second is dissolving and incongruently dissolving of this minerals when manuring is precluded. The manuring intensity varying in time and variable atmospheric precipitation, both resulting in periodically changing chemical composition of ornithogenic waters, determine the commonly two- or three-phase phosphate composition in individual soil samples.

Specific feature of the described minerals in comparison with the other described in literature is the high content of organic carbon. Besides the known tendency of phosphates to compound formation with simple organic groups (Lewis Scharpf 1973), the presence of organic remains should be also taken into account (Fig. 23, 24, 25 and 26). Forms presented in Fig. 23 are most common.

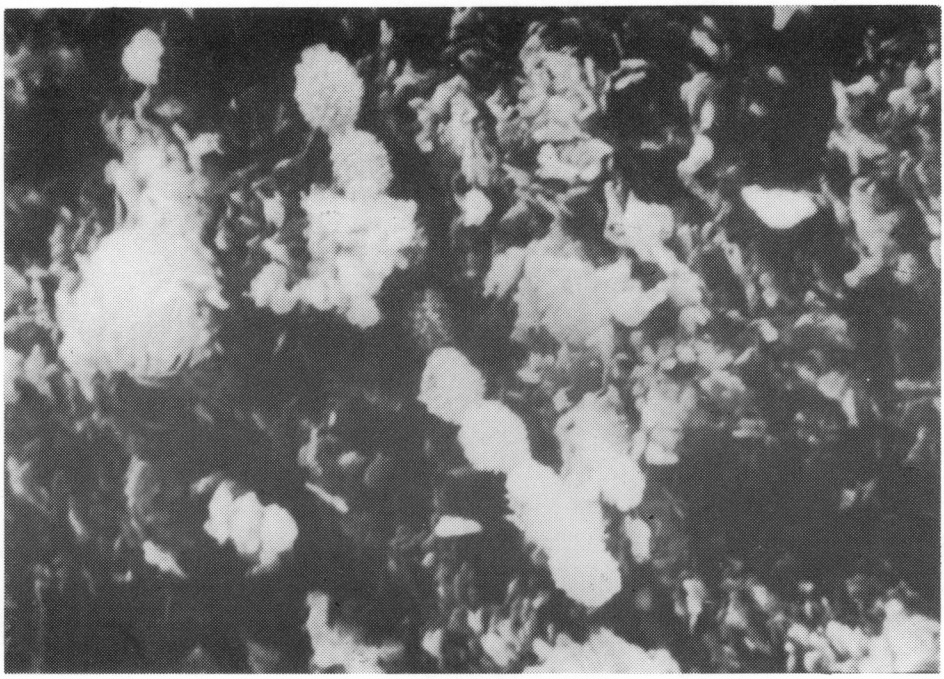

Fig. 23. Taranakite — structure of crystal aggregates
Unindentified organic form is visible in the center. Sceanning electron microscope image, magnification 2390x

Photo A. Tatur, A. Barczuk

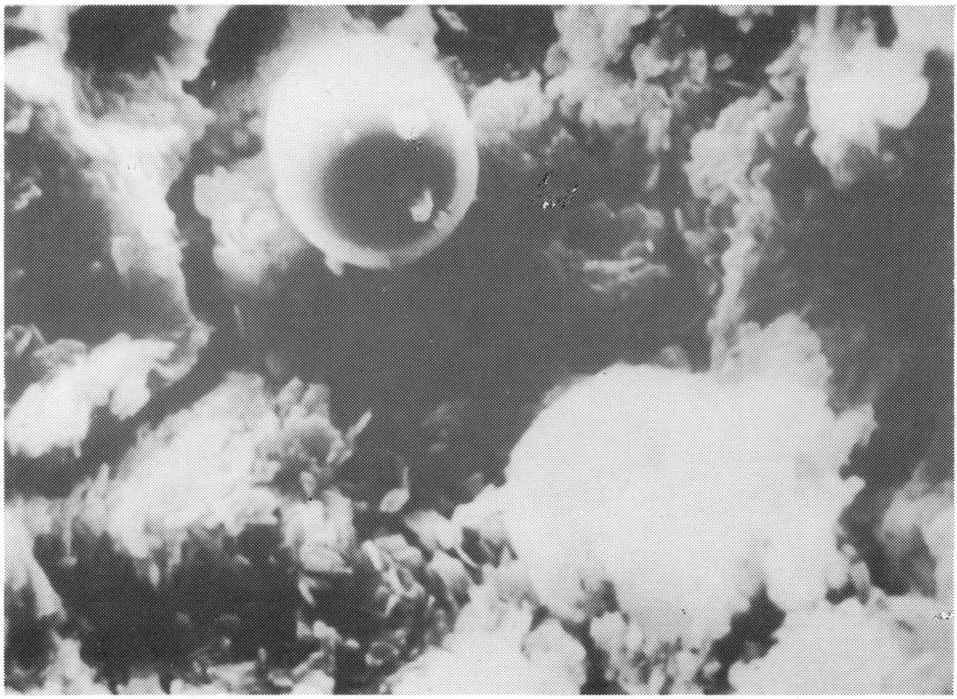

Fig. 24. Taranakite — structure of crystal aggregate
In the upper part the unidentified spherical organic form is visible. Scanning electron microscop, image, magnification 3980x

Photo A. Tatur, A. Barczuk

Fig. 25. Taranakite. Flaky structure of crystal aggregate, locally hexagonal habit is discernible. Scanning electron microscope image, magnification 9610 ×

Photo A. Tatur, A. Barczuk

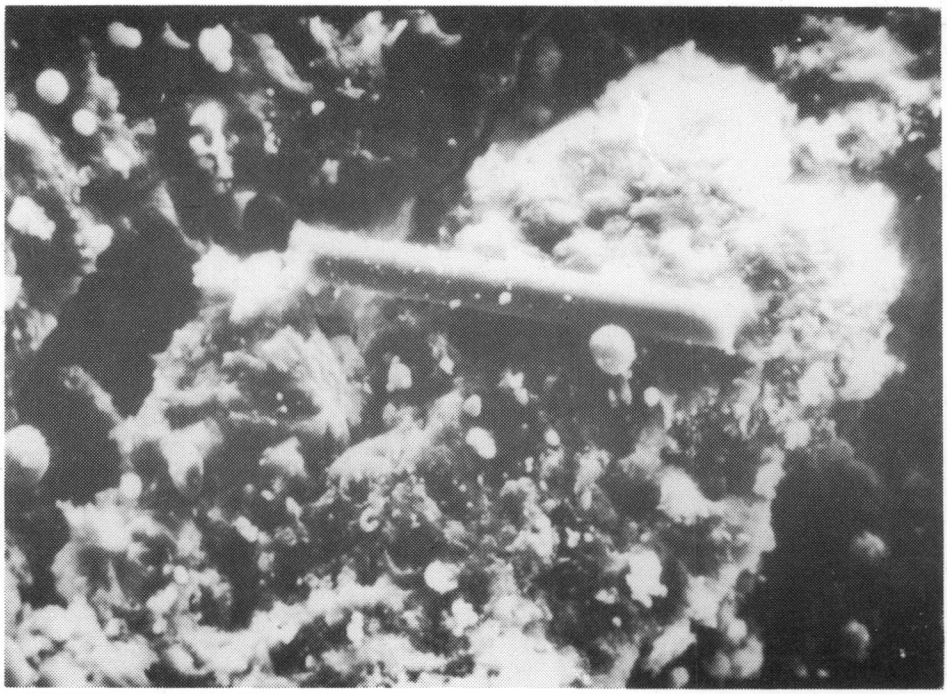

Fig. 26. Numerous organic forms of spherical small and bacilliform (large) habit on the cleavage surface of minyulite
Scanning electron microscope image, magnification 1200x

Photo A. Tatur, A. Barczuk

The authors would like to thank Prof. Dietrich Adelung for render determinations of fluorine in phosphates accesible. Thanks are extended to Dr. Piotr Dzierżanowski, Michał Kuźniarski M. Sc. for help in petrographical analysis and to Mrs Danuta Malanowska for participation in preparing of the manuscript.

6. Резюме

Исследования были проведены в районе залива Адмиралты на острове Кинг Джордж (Южные Шетланды) во время антарктического лета на переломе 1979 на 1980 год. В работе проанализованы минералы, находящиеся в гуано колонии пингвинов и в нижележащих каменистых и глинистых моренных и делювиальных отложениях, которые были фосфатизированы промывающими гуано растворами. Морены и делювия были образованы в процессе выветривания основных вулканических пород, прежде всего андезитов и базальтов, формирующих остров. Были исследованы образцы характерные для разнородного в минералогическом смысле района, собранные во время исследований орнитогенных почв (Татур и Мырха 1983). Места отбора образцов для минералогических исследований обозначены на рисунках 1—4. Для определения минералогического состава фосфатных пород были выполнены рентгенографические (рис. 6, таблица IV), химические (таблица II), петрографические и минералогические с использованием поляризационного и сканирующего электронного микроскопов (рис. 8—26) а также термогравиметрические (рис. 7) исследования.

Были определены следующие минералы: в гуано — струвит и гидроксилапатит, в фосфатизированной зоне — лейкофосфит, миниюлит, аморфический фосфат аммония и на некотором расстоянии от орнитогенных почв — вивианит.

Распределение охарактеризованных фосфатов в вертикальной колонке (таблица III) является результатом метаморфоза химического состава вод промывающих гуано и после этого фильтрующихся сквозь почву. Воды, стекающие с колонии пингвинов по поверхности почв, являются щелочными или нейтральными и содержат переменные, часто очень высокие концентрации минеральных соединений фосфора и азота с отчётливым превосходством аммониевого азота над нитратным. После фильтрации сквозь почву химический состав вод стабилизируется и воды становятся кислыми (pH 4 или несколько выше), а нитраты количественно превосходят аммониевый ион (таблица I).

Струвит находится исключительно на поверхности почв. Этот минерал кристаллизуется из щелочных вод богатых аммиаком и в некоторой степени — магнием.

Гидроксилапатит находится повсеместно во всем поверхностном слое гуано, где он является главным минералом, возникающим из минерализующегося органического вещества фекалий пингвинов, содержащих почти исключительно раздробленные остатки криля.

Лейкофосфит находится в самом неглубоком горизонте фосфатной зоны, доходящим до поверхности почв или залегающим под тонким слоем гуано. Он образуется как осадок из нейтральных и слабокислых растворов богатых аммониевым ионом. Временное просушивание и насыщение кислородом этого слоя способствует окислению железа до Fe^{+3}, и следовательно кристаллизации этого минерала.

Миниюлит характерен для более глубокого слоя, где он образуется в процессе метасоматических реакций между раствором и силикатной фазой почвы. Не исключено, что важную роль в образовании этого минерала играют высокие концентрации питательного вещества и фтора в орнитогенных водах.

Таранакит характерен для самых глубоких, всегда насыщенных водой слоев. Он возникает путём осаждения из кислых и очень разбавленных растворов.

Лейкофосфит, миниюлит и таранакит возникают и являются стабильными в присут-

ствии растворов с высокой концентрацией щелочей. Когда воды фильтрирующие через почву содержат мало щелочей и временно падает общая концентрация растворенных ионов (например во время обильных осадков или таяния снегов и льда), образуется простой аморфный фосфат алюминия. Он может возникать как продукт непосредственных метасоматических реакций раствора с твёрдой фазой или путём инконгруэнтного растворения минералов, содержащих калий. Более кислые условия, периодически существующие в растворах, могут быть причиной кристаллизации замеченных в скоплениях аморфного фосфата алюминния малых количеств форм, похожих на варисцит.

7. Streszczenie

Badania przeprowadzono w rejonie Zatoki Admiralicji na Wyspie Króla Jerzego (Szetlandy Południowe), podczas lata antarktycznego na przełomie lat 1979/1980. W pracy analizowano minerały występujące w guanie pingwinisk, oraz podległych sfosfatyzowanych przez roztwory płuczące guano, kamienistych i gliniastych utworach morenowych i deluwialnych, pochodzących z wietrzenia zasadowych skał wulkanicznych (głównie andezyty i bazalty) budujących tę wyspę. Badano próbki które wytypowane zostały jako charakterystyczne dla zróżnicowania mineralogicznego, podczas badań gleb ornitogennych na tym terenie (Tatur and Myrcha 1983). Miejsca pobrania próbek zaznaczone są na rysunkach 1—4. W celu identyfikacji mineralogicznej, wykonano analizy rentgenograficzne (rys. 6, tabela IV), składu chemicznego (tabela II), przedstawiono w tekście dane dotyczące cech optycznych oznaczonych w mikroskopie polaryzacyjnym, dokonano obserwacji w mikroskopie scanningowym (rys. 8—26) dla wybranych próbek, przedstawiono również wyniki analizy termograwimetrycznej (rys. 7).

W guanie znaleziono struwit, hydroksylapatyt, w strefie sfosfatyzowanej: leukofosfit, minyulit, amorficzny fosforan glinu taranakit, oraz w pewnym oddaleniu od gleb ornitogennych — wiwianit.

Rozmieszczenie opisanych fosforanów w profilu pionowym (tabela III) wynika z metamorfozy składu chemicznego wód przemywających guano i przesiąkających przez te gleby. Wody spływające z pingwiniska po powierzchni gleb są alkaliczne lub obojętne, charakteryzują się zmiennymi, często bardzo wysokimi koncentracjami mineralnych form fosforu i azotu, ze zdecydowaną dominacją formy amonowej nad azotanową. Po perkolacji przez glebę, skład chemiczny ulega stabilizacji, a odczyn staje się kwaśny (pH 4 lub nieco wyższe). Wśród mineralnych form azotu, azotany przeważają nad formą amonową (tabela I).

Struwit obecny jest wyłącznie na powierzchni gleb; krystalizuje z wód alkalicznych bogatych w amoniak i wzbogaconych w magnez.

Hydroksylapatyt powszechny jest w całej warstwie powierzchniowej guana, gdzie jest głównym minerałem powstającym z mineralizującej się materii organicznej fekaliów pingwinich składających się niemal wyłącznie z rozdrobnionych resztek kryla.

Leukofosfit występuje w najpłytszym horyzoncie strefy sfosfatyzowanej, dochodzącym do powierzchni gleb, lub zalegającym tuż pod cienką warstwą guana. Powstaje on jako precypitat z roztworów obojętnych i słabo kwaśnych, zasobnych jeszcze w jon amonowy. Okresowe przesuszanie i natlenienie tej warstwy sprzyja obecności Fe^{III}, występującego w strukturze krystalicznej tego minerału.

Minyulit charakterystyczny jest dla warstwy głębszej, gdzie powstaje jako produkt metasomatycznych reakcji między roztworami a fazą krzemianową gleby. Niewykluczone, że istotną rolę w powstaniu tego minerału odgrywa odpowiednio wysokie stężenie nutrientów, oraz fluoru w ornitogennych wodach.

Taranakit jest charakterystyczny dla najgłębszych, zawsze mokrych poziomów. Powstaje on jako precypitat z roztworów kwaśnych i najbardziej rozcieńczonych.

Leukofositt, minyulit i taranakit powstają i są trwałe w obecności roztworów o wysokiej

koncentracji alkaliów, natomiast gdy wody przesiąkające przez glebę zawierają niską koncentrację alkaliów, lub są okresowe słabo zmineralizowane (np. wody opadowe i roztopowe) tworzy się prosty amorficzny fosforan glinu. Może on powstawać jako produkt bezpośrednich metasomatycznych reakcji między roztworem a fazą stałą, a może też być produktem inkongruentnego rozpuszczania minerałów zawierających potas. Okresowe panujące w roztworach warunki bardziej kwaśne, mogą być przyczyną obserwowanych w obrębie amorficznego fosforanu glinu, niewielkich ilości form krystalicznych waryscyto-podobnych.

8. References

1. Altschuler Z. S. 1973 — The weathering of phosphate deposits — geochemical and environmental aspects (In: Environmental Phosphorus Handbook, Eds. E. J. Griffith, A. Beeton, J. M. Spencer and D. T. Mitchell) J. Wiley and Sons, New York, London, Sydney, Toronto, 33—96.
2. Arlidge E. Z., Farmer V. G., Mitchell B. D., Mitchell W. A. 1963 — Infra-red, x-ray thermal analysis of some aluminum and ferric phosphates — J. appl. Chem., Lond., 13: 17—27.
3. ASTM 1967 — Inorganic idex to the powder diffraction File — American society for testing and materials 1916, Race Street, Philadelphia, Pa. 19103.
4. Axelrod J. M., Carran M. K., Milton C., Thayer T. P. 1952 — Phosphate mineralization at Bomi Hills and Bambuta Liberia, West Africa — Am. Mineral., 37: 883—909.
5. Bache B. W. 1963 — Aluminium and iron phosphate studies relating to soils. I. Solution and hydrolysis of variscite and strengite — J. Soil Sci., 14: 113—123.
6. Bannister F. A., Hutchinson G. E. 1947 — The identity of minervite and palmerite with taranakite — Mineral. Mag., 28: 31—35.
7. Belopol'skij M. P., Bumakova N. J., Gumbar K. K., Mihailova N. A., Popov N. P. 1974 — Analiz fosfatov (In: N. P. Popov: Himičeskij analiz gornyh porod i mineralov Nedra, Moskva 209—225.
8. Birkenmajer K. 1980 — Geology of Admiralty Bay, King George Island (South Shetlands Islands) — An outline — Pol. Polar Res., 1, (1): 29—54.
9. Birkenmajer K. 1981 — Raised marine features and glacial history in the vicinity of H. Arctowski Station, King George Island (South Shetlands Islands, West Antarctica) — Bull. Ac. Pol. Sci. Ser. A, 29: 109—117.
10. Bridge P. J. 1971 — Analyses of altered struvite from Skiton, Victoria — Mineral. Mag. 38: 381—382.
11. Brown W. E. 1973 — Solubilities of phosphates and other sparingly soluble compounds — (In: Environmental phosphorous Handbook Eds. E. J. Griffith, A. Beeton, J. M. Spencer and D. T. Mitchell) — J. Wiley and Sons, New York, London, Sydney, Toronto, 203—263.
12. Chester G., Allen O. N., Attoe O. J. 1959 — Differential thermograms of selected organic acids and derivatives — Proc. Soil Sci. Soc. Am., 23: 454—457.
13. Cole C. V., Jackson M. L. 1950 a — Colloidal dihydroxy dihydrogen phosphates of aluminum and iron with crystalline character established by electron and X-ray diffraction — J. Phys. Chem., 54: 128—142.
14. Cole C. V., Jackson M. L. 1950 b — Solubility equilibrium constans of dihydroxy — aluminum dihydrogen phosphate relating to a mechanism of phosphate fixation in soils — Soil Sci. Soc. Am. 84—89.
15. Fisher D. J. 1973 a — Geochemistry of minerals containing phosphorus. In: Environmental phosphorus Handbook Eds. E. J. Griffith, A. Beaton, J. M. Spencer and D. T. Mitchell) — J. Wiley and Sons, New York, London, Sydney, Toronto, 141—152.
16. Fischer D. J. 1973 b — Identification of phosphorus-bearing minerals. (In: Environmental

phosphorus Handbook Eds. E. J. Griffith, A. Beeton, J. M. Spencer and D. T. Mitchell) — J. Wiley and Sons, New York, London, Sydney, Toronto, 153—168.
17. Frondel C. 1958 — Geochemical scavening of strontium — Science 128: 1623—1624.
18. Frondel C., Ito J., Montgomery A. 1968 — Scandium content of some aluminum phosphates — Am. Mineral. 53: 1223—1231.
19. Haseman I. F., Brown E., Whitt C. D. 1950 a — Some reactions of phosphate with clays and hydrous oxides of iron and aluminum — Soil Sci. 70: 257—271.
20. Haseman J. F., Lehr J. R., Smith J. P. 1950 b — Mineralogical character of some iron and aluminum phosphates containing potassium and ammonium — Soil Sci. Soc. Am. Proc., 15: 76—84.
21. Hsu P. H. 1982 — Crystallization of variscite at room temperature — Soil Sci., 133/5: 305—313.
22. Hsu P. H., Jackson M. L. 1960 — Inorganic phosphate transformations by chemical weathering in soils as influenced by pH — Soil Sci. 90: 16—24.
23. Hutchinson G. E. 1950 — Biogeochemistry of vertebrate excretion — Bull. Amer. Mus. Nat. Hist., 96: 1—554.
24. Jabłoński B. 1984 — Distribution and numbers and breeding preference of penguins in the region of Admiralty Bay (King George Island, South Shetlands) in the season 1979/1980 — Pol. Polar Res., 5:
25. Kittrick J. A., Jackson M. L. 1955 — Application of solubility product principles to the variscite-koalinite system — Soil Sci. Am. Proc., 19: 455—457.
26. Koch S., Sarudi J. 1964 — The hydrous basic aluminium phosphates of Zeležnik (Vašegy), Slovakia (CSSR) — Acta Min. Petr. Unv. Szeged., 16: 3—10.
27. Langmyhr F. J., Paus P. E. 1968 — The analysis of inorganic siliceous materials by atomic absorption spectrophotometry and the hydrofluoric acid decomposition technique. Part III-The analysis of bauxite — Anal. Chim. Acta, 43: 508—510.
28. Larson E. S., Berman H. 1934 — The microscopic determination of the non-opaque minerals — Washington (in Russian II ed.) Petrov ONTJ Moskva 1965, 462 pp.
29. Levis G., Scharpf J. R. 1973 — Transformation of naturally occurring organophosphorus compounds in the environment — (In: Environmental Phosphorus Handbook Eds. E. J. Griffith, A. Beeton, J. M. Spencer and D. T. Mitchell) — J. Wiley and Sons, New York, London, Sydney, Toronto, 393—412
30. Lindberg M. L. 1957 — Leucophosphite from the Sapucaia pegmatite mine, Minas Gerais, Brazil — Amer. Min., 42: 214—221.
31. Maciołek J. A. 1972 — Limnological organic analysis by quantitative dichromate oxidation — Bureau of Sport Fisheries and Wildlife Publication, 61 pp.
32. Marczenko Z. 1979 — Spektrofotometryczne oznaczanie pierwiastków — PWN, Warszawa, 757 pp.
33. Moczydłowski G. 1978 — Charakterystyka procesów atmosferycznych i klimatu rejonu Stacji im. H. Arctowskiego w Antarktyce — Kosmos A, 2: 189—198.
34. Murray J. W., Dietrich R. K. 1956 — Brushite and taranakite from Pog Hole Cave, Giles, Co. Virginia — Am. Mineral., 41: 616—626.
35. Palache C., Berman H., Frondel C. 1951 — Dana's system of mineralogy — 7-th Ed. Vol. 2 1951 — Wiley, New York, 1124 pp.
36. Penkala T. 1977 — Zarys krystalografii (II wydanie) — PWN, Warszawa, 467 pp.
37. Rantala R. T. T., Loring D. H. 1975 — Multielement analysis of silicate rocks and marine sediments by atomic absorption spectrophotometry — Atomic Absorption Newsletter, 15 (5): 117—120.
38. Smith J. P., Brown W. E. 1959 — X-ray studied of aluminum and iron phosphates containing potassium or ammonium — Am. Mineral., 44: 138—142.
39. Solorzano L. 1962 — Determination of ammonia in natural water by the phenol-hypochlorite method — Limnol. Oceanogr., 14: 799—801.

40. Spencer L. J., Bannister F. A., Hey M. M., Bennet H. 1943 — Minyulite (hydrous K — Al fluophosphate) from South Australia — Mineral. Mag., 26: 309—314.
41. Strickland J. D. H., Parsons T. R. 1968 — A Practical Handbook of Seawater Analysis — Fish Res. Bd. (Canada) Bull. 167, Ottawa.
42. Stumm W., Morgan J. J. 1970 — Aquatic chemistry. An introduction emphasizing chemical equilibria in natural waters — Viley, New York, London, Sydney, Toronto, 583 pp.
43. Simmons G. C. 1964 — Leucophosphorite a new occurrence in the Quadrilatero Ferrifero, Minas Gerais, Brazil — Am. Mineral. 49: 377— 386.
44. Simpson C. S. 1931-32 — Contribution of Western Australia — Roy. Soc. West. Australia J., 18: 61—71.
45. Swanson H. E., Morris M. C., Evans E. H., Ulmer L. 1964 — Standard X-ray diffraction powder patterns — National Bureau Standards Monogr. 25, sect. 3.
46. Stefanovič P. 1957 — Investigation of humus substances on the basis of DTA curves — Agrokem. Talait., 6: 129—136.
47. Szpila K., Chlebowski R., Pelc A., Stępisiewicz M., Wichrowski Z. 1982 — Mineralogia kamieni nerkowych — Archiwum mineralogiczne 38: 89—94.
48. Tatur A., Barczuk A. 1984 — Ornithogenic minerals on King George volcanic Island — Polar Biol.
49. Tatur A., Myrcha A. 1983 — Changes of chemical composition of waters running of from penguin rookeries on King George Island (Maritime Antarctic) — Pol. Polar Res., 4: 113—128.
50. Tatur A., Myrcha A. 1984 — Ornithogenic soils on King George Island, South Shetland Islands (Maritime Antarctic) — Pol. Polar. Res., 5: 31—60.
51. Taylor A. W. 1963 — Potassium and ammonium taranakites, amorphous aluminum phosphate and variscite as sources of phosphate for plants — Soil Sci. Soc. Am. Proc., 27: 148—151.
52. Taylor A. W., Gurney E. L., Lindsay W. L. 1960 — An evaluation of some iron and aluminum phosphates as sources of phosphate for plants — Soil Sci., 90: 25—38.
53. Taylor A. W., Gurney E. L. 1961 — Solubilities of potassium and ammonium taranakites — J. Phys. Chem., 56: 1613—1616.
54. Taylor A. W., 1962 — Solubility of aluminum phosphate — Soil Sci., 93: 241—245.
55. Van Wazer J. R. 1961 — Phosphorous and its compounds — Interscience Publishers, New York. vol. II.
56. Vasiler E. K., Kašaeva G. M., Uščapovskaja Z. G. 1974 — Rentgenometričeskij opredelitel' mineralov (klass fosfatov) — Nauka, Moskva.
57. Ward D. A., Biechler D. G. 1975 — Rapid direct determination of calcium in natural waters by Atomic Absorption Spectrometry — Atom, Abs. Newsl., 14 (1): 29—31.
58. White W. C., Warin O.N. 1964 — A survey of phosphate deposits in the Southwest Pacific and Australian Waters — Bureau Min. Res. Aust. Bull., 69: 1—173.
59. Wilson M. J., Bain D. D. 1976 — Occurence of leucophosphite in a soil from Elephant Island, British Australia Territory — Am. Mineral., 61: 1027—1028.
60. Zubek K. 1980 — Climatic conditions at the Arctowski Station (King George Island, South Shetland Islands) in 1977 — Pol. Arch. Hydrobiol., 27: 235—244.

Paper received 30 November 1983